

Multiple Binding Sites for Melatonin on Kv1.3

Zoltán Varga,* György Panyi,* Mózes Péter, Jr.,* Carlo Pieri,[†] György Csécséi,[‡] Sándor Damjanovich,* and Rezső Gáspár, Jr.*

*Department of Biophysics and Cell Biology, University Medical School of Debrecen, Debrecen H-4012, Hungary; [†]Cytology Center, Research Department of Gerontology, Ancona 60121, Italy; and [‡]Department of Neurosurgery, University Medical School of Debrecen, Debrecen H-4012, Hungary

ABSTRACT Melatonin is a small amino acid derivative hormone of the pineal gland. Melatonin quickly and reversibly blocked Kv1.3 channels, the predominant voltage-gated potassium channel in human T-lymphocytes, acting from the extracellular side. The block did not show state or voltage dependence and was associated with an increased inactivation rate of the current. A half-blocking concentration of 1.5 mM was obtained from the reduction of the peak current. We explored several models to describe the stoichiometry of melatonin-Kv1.3 interaction considering one or four independent binding sites per channel. The model in which the occupancy of one of four binding sites by melatonin is sufficient to block the channels gives the best fit to the dose-response relationship, although all four binding sites can be occupied by the drug. The dissociation constant for the individual binding sites is 8.11 mM. Parallel application of charybdotoxin and melatonin showed that both compounds can simultaneously bind to the channels, thereby localizing the melatonin binding site out of the pore region. However, binding of tetraethylammonium to its receptor decreases the melatonin affinity, and vice versa. Thus, the occupancy of the two separate receptor sites allosterically modulates each other.

INTRODUCTION

Specific peptide and nonpeptide channel blockers are widely used to investigate the function of Kv1.3 and the molecular mechanism of its operation (Aiyar et al., 1995). Based on the mechanism of block there are two groups of blockers in general: pore blockers and gating modifiers (Hille, 1992). Pore blockers inhibit the K^+ current by plugging the pore of the channel. Peptide toxins such as charybdotoxin (ChTx) and those of the scorpion *Pandinus imperator* belong to this group; they bind to the channels with 1:1 stoichiometry (Goldstein and Miller, 1993; Péter et al., 1998). ChTx is a widely used pore blocker, which binds to both voltage-gated and Ca^{2+} activated K^+ channels with high affinity (Goldstein and Miller, 1993; MacKinnon and Miller, 1988). Tetraethylammonium (TEA) is a quaternary ammonium compound with a pore-blocking mechanism similar to that of peptide toxins (Spruce et al., 1987; Yellen et al., 1991).

Gating modifiers such as hanatoxin (HaTx) block the K^+ current by modifying the gating mechanism of the channel. HaTx shifts the channel opening to more depolarized membrane potentials. One HaTx molecule can bind to each of the four subunits of the channel (Swartz and MacKinnon, 1997a, b).

Some channel blockers have only intracellular binding sites, but they still have an effect when they are applied from the extracellular side. Extracellularly applied 4-ami-

nopyridine passes through the membrane in its nonionized form and acts in its ionized form from the intracellular side. The binding site of 4-aminopyridine is on the S5 and S6 transmembrane segments (Rasmusson et al., 1995). The mechanism of block by clofilium, a quaternary ammonium compound with antiarrhythmic effect, was studied on human Kv1.5 delayed rectifier potassium channels (Malayev et al., 1995). Clofilium penetrates the membrane; its binding site is at the intracellular side of the channel close to the pore, and it can be trapped in the channel when the channel closes.

Voltage-gated potassium channels have two binding sites for TEA: one on the intracellular and another one on the extracellular side (MacKinnon and Yellen, 1990; Yellen et al., 1991; Kirsch et al., 1991; Heginbotham and MacKinnon, 1992). TEA binds to the channel with 1:1 stoichiometry and plugs the pore of the channel from both sides. The intracellular and extracellular binding sites for TEA are on the linker between S5 and S6. The intracellular binding site is in the electric field of the membrane 25% deep from the cytosol causing a voltage-dependent block; however, the extracellular site is more superficial, showing no or mild voltage dependence of the block (Heginbotham and MacKinnon, 1992). At the extracellular TEA binding site the rate of block and unblock is extremely fast, resulting in a reduction of the single-channel current amplitudes (Kirsch et al., 1991).

Recently, it has been shown that melatonin (*N*-acetyl-5-methoxytryptamine, Fig. 1), the main hormone of the pineal gland, is likely to interact with ion channels at the cell membrane and influence the membrane potential (Wanecsek and Klein, 1992; Pieri et al., 1998; Jiang et al., 1995; Oreslock, 1984; Pioli et al., 1993). An inhibitory effect of melatonin has also been observed on the proliferation of

Received for publication 15 April 1999 and in final form 1 December 2000.

Address reprint requests to Dr. Rezső Gáspár, Jr., Department of Biophysics and Cell Biology, University Medical School of Debrecen, Nagyterdei krt. 98, Debrecen H-4012, Hungary. Tel.: 36-52-412-623; Fax: 36-52-623; E-mail: gaspar@jaguar.dote.hu.

Zoltán Varga and György Panyi are equally considered as first author.

© 2001 by the Biophysical Society

0006-3495/01/03/1280/18 \$2.00

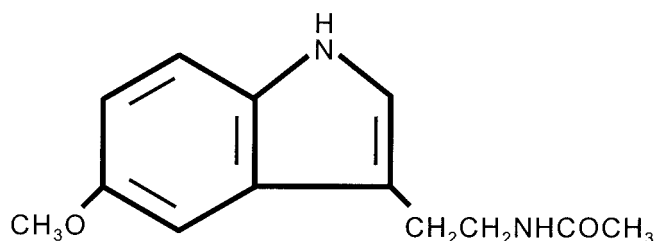


FIGURE 1 The chemical structure of melatonin.

human lymphocytes and lymphoid cells (Persengiev and Kyurkchiev, 1993; Vijayalaxmi et al., 1996).

In view of these observations and the involvement of Kv1.3 channels in lymphocyte activation, the effect of extracellular melatonin has been studied on the Kv1.3 channels of human peripheral blood T lymphocytes by the patch-clamp method.

Due to the possible role of melatonin in immunological processes (see Liebmann et al., 1997, for review) our initial goal was to find a detectable interaction of melatonin with ion channels of T cells at its physiological concentration (200 pM; Liebmann et al., 1997). However, observable effects were only seen at concentrations several orders of magnitude higher than the physiological range. The effective concentration range was found to be similar to that applied in the studies demonstrating the influence of melatonin on the membrane potential and proliferation of lymphocytes. Although this renders the physiological relevance of this interaction unlikely, the unusual characteristics of the blocking mechanism are worth investigating.

Here we show that melatonin, an amino acid derivative, blocks Kv1.3 channels in a reversible manner. During the block the drug-channel interaction is characterized by a 4:1 binding stoichiometry and not by a simple pore-blocking mechanism. Part of this work has been published in abstract form (Varga et al., 1999).

MATERIALS AND METHODS

Cells

Heparinized human peripheral venous blood was obtained from healthy volunteers. Mononuclear cells were separated by Ficoll-Hypaque density gradient centrifugation. Collected cells were washed twice with Ca²⁺ and Mg²⁺ free Hanks' solution containing 25 mM HEPES (pH 7.4). Cells were cultured in a 5% CO₂ incubator at 37°C in 24-well culture plates in RPMI-1640 supplemented with 10% FCS (Hyclone, Logan, UT), 100 U/ml penicillin, 100 μg/ml streptomycin, and 2 mM L-glutamine at 0.5 × 10⁶/ml density for 3–4 days. The culture medium also contained 2.5 or 5 μg/ml phytohemagglutinin A (PHA-P, Sigma-Aldrich Kft, Budapest, Hungary) to increase K⁺ channel expression (Deutsch et al., 1986, 1991).

Cytotoxic murine T cells (CTLL-2) were transiently co-transfected with plasmids encoding a mutated (pRc/CMV/H399Y) Kv1.3 channel along with a Ccd4neo plasmid (gifts from Dr. Carol Deutsch, University of Pennsylvania, Philadelphia, PA), containing the gene for human membrane-surface CD4, at a molar ratio of 5:1 or 8:1 [32 or 48 μg/ml total

DNA] using electroporation (Deutsch and Chen, 1993). CTLL-2 cells were cultured in RPMI-1640 supplemented with 10% FBS (Hyclone, Logan, UT), 2 mM sodium pyruvate, 10 mM HEPES, 4 mM L-glutamine, 50 μM 2-mercaptoethanol, and 100 CU/ml IL-2. Before transfection, cells were cultured for 24 h in fresh medium and collected in the logarithmic phase of growth. After harvesting, cells were suspended in Hanks' 20 mM HEPES balanced salt solution (pH = 7.23) at 2 × 10⁷ cells/ml, and the appropriate mixture of DNA was added to the cell suspension. This suspension was transferred to electroporation cuvettes (400 μl/cuvette, 4 mm electrode gap), kept on ice for 10 min, and then electroporated using a BTX electroporator (San Diego, CA) with settings previously determined to give ~50% viability at 24 h posttransfection (725 V/cm, 2200 μF, 13 Ω). The resultant time constants were 24–25 ms. Cells were incubated for an additional 10 min on ice, and transferred back to culture medium (~0.5 × 10⁶ cells/ml) supplemented with 5 mM sodium butyrate (at 37°C, 5% CO₂). Cells were used for electrophysiology between 8 to 16 h after transfection.

Electrophysiology

Whole-cell and single-channel measurements were carried out using Axopatch-200 and Axopatch-200A amplifiers connected to personal computers using Axon Instruments TL-1-125 and Digidata 1200 computer interfaces, respectively. For data acquisition and analysis the pClamp6 software package (Axon Instruments Inc., Foster City, CA) was used. T lymphocytes and CD4⁺ CTLL-2 cells were selected for current recording by incubation with mouse anti-human CD2 (Becton-Dickinson, San Jose, CA) and mouse anti-human CD4 antibodies (0.5 μg/10⁶ cells, AMAC, Westbrook, ME), respectively, followed by selective adhesion to petri dishes coated with goat anti-mouse IgG antibody (Biosource, Camarillo, CA), as previously described by Matteson and Deutsch (1984) and Deutsch and Chen (1993). Dishes were washed gently five times with 1 ml normal extracellular bath medium (see below) before the patch-clamp experiments. Standard whole-cell patch-clamp techniques were used, as described previously (Matteson and Deutsch, 1984). Pipettes were pulled from GC 150 F-15 borosilicate glass capillaries (Clark Biomedical Instruments, Pangbourne, UK) in two stages and fire-polished to give electrodes of 2–3 MΩ resistance in the bath. The normal bath solution was (in mM): 145 NaCl, 5 KCl, 1 MgCl₂, 2.5 CaCl₂, 5.5 glucose, 10 HEPES (pH 7.35, 305 mOsm). For CTLL-2 cells the bath solution also contained recombinant interleukin-2 (8.3 ng/ml). The pipette solution was (in mM): 140 KF, 11 K₂EGTA, 1 CaCl₂, 2 MgCl₂, and 10 HEPES (pH 7.20, ~295 mOsm).

Test substances

Melatonin (Sigma-Aldrich Kft) stock solution was prepared in DMSO (200 mM). Bath solutions with different melatonin concentrations were prepared freshly before the experiments. Appropriate control bath solutions contained equal DMSO concentration to the test solution. The normal bath solution prepared this way was referenced as control in the paper unless stated otherwise (see below). The maximal DMSO concentration was 5% v/v. Different TEA-Cl solutions were prepared by equimolar substitution of NaCl with TEA-Cl. In high K⁺ solution, NaCl was completely substituted by KCl (150 mM KCl final concentration). Charybdotoxin (Alamone Labs Ltd., Jerusalem, Israel) was dissolved in normal bath solution supplemented with 0.1 mg/ml bovine serum albumin (Sigma-Aldrich Kft).

Bath perfusion with different test solutions was achieved using a gravity-flow perfusion setup with eight input lines and a PE10 polyethylene tube output tip with flanged aperture to reduce turbulence of the flow. Solutions were applied in an alternating sequence of control and test solutions unless stated otherwise. Excess fluid was removed continuously from the bath.

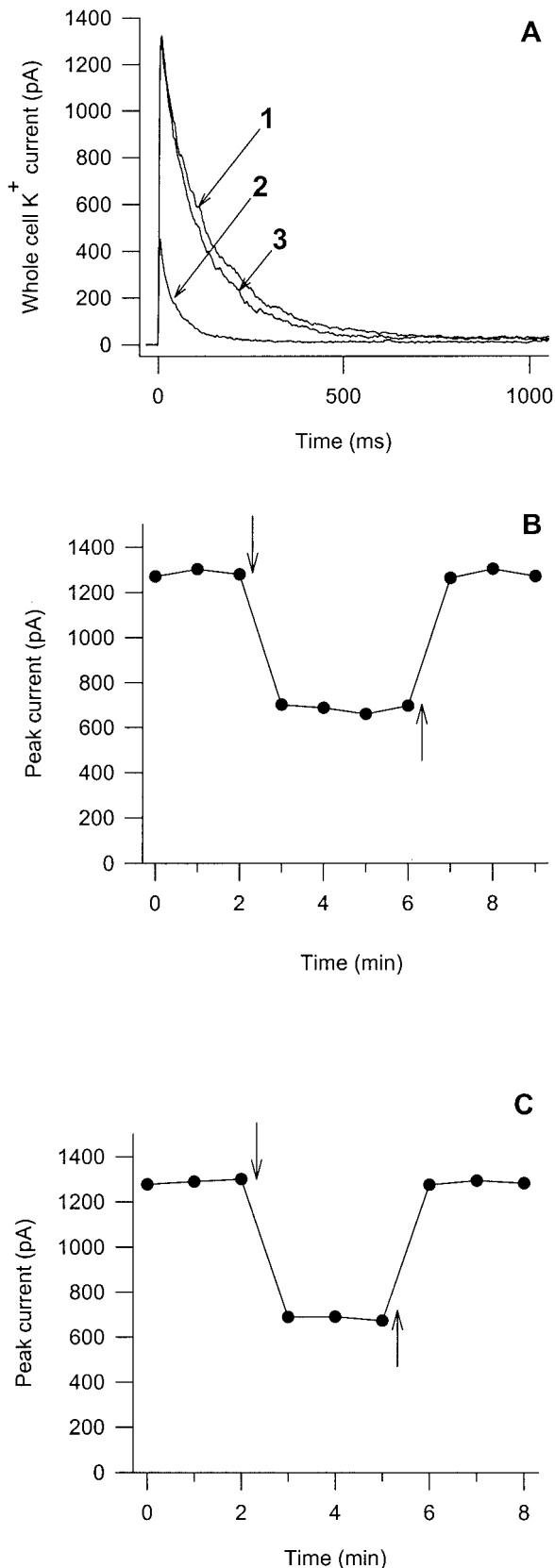


FIGURE 2 Melatonin reversibly blocks Kv1.3 channels. (A) Whole-cell K^+ currents of a human peripheral T lymphocyte recorded during 2-s-long test pulses to +40 mV from a holding potential of -120 mV. Test pulses

Data analysis

Before analysis whole-cell current traces were corrected for ohmic leak and digitally filtered (3-point boxcar smoothing). Nonlinear least-squares fits were done using the Marquardt-Levenberg algorithm. Fits were evaluated visually by the residuals and the sum of squared differences between the measured and calculated data points.

Single-channel traces were digitally filtered using 400 Hz Gaussian filtering. Traces that contained no channel openings were averaged and this average current was subtracted from each trace to subtract capacitive and leakage currents. Short regions at the beginning of traces were not included in the analysis to leave out noisy multiple openings. All-points histograms were fitted with the sum of Gaussian distributions using the least-squares technique.

Statistical comparisons were made using Student's *t*-test, and when appropriate, paired *t*-test or ANOVA at $p = 0.05$. For all experiments the standard error of the mean (SE) is reported.

RESULTS

Block of Kv1.3 channels by melatonin

Fig. 2 illustrates that upon depolarization to +40 mV test potential from a holding potential of -120 mV human T lymphocytes display outward whole-cell currents under the applied experimental conditions. This quickly activating and slowly inactivating current has been identified as potassium current flowing through voltage-gated ion channels designated Kv1.3 (Matteson and Deutsch, 1984; Decoursey et al., 1984). The amplitude of the potassium current is considerably reduced during perfusion of the bath with extracellular solution containing 2 mM melatonin, as shown in Fig. 2 A. In addition, the rate of inactivation of the whole-cell current is also increased by melatonin. Both the amplitude of the whole-cell current and the inactivation time constant returned to the control value when the extracellular bath was reperused with drug-free bath solution (apart from a negligible inherent acceleration of inactivation with time after achieving whole-cell configuration).

Development of and recovery from current inhibition was studied using short (50-ms) pulses to +40 mV (Fig. 2 B) applied every 60 s. This pulse rate did not cause cumulative

were applied every 90 s. The bath was perfused with (1) control solution, (2) a solution containing 2 mM melatonin, (3) control solution again. During the experiment excess fluid was removed by continuous suction. Sampling and low-pass filter frequencies were 2000 and 1000 Hz, respectively. Off-line leak subtraction and 3-point boxcar smoothing were applied. (B) Whole-cell peak currents of a human T lymphocyte during the administration and washout of 1.5 mM extracellular melatonin. Test pulses to +40 mV (50 ms duration) were applied every 60 s. Continuous perfusion was applied with control solution before the down arrow, with the same solution containing 1.5 mM melatonin after the down arrow, and with control fluid again after the up arrow. Off-line leak subtraction and 3-point boxcar smoothing were used. Sampling and low-pass filter frequencies were 20 and 5 kHz, respectively. (C) The same experimental arrangement as for B but 1-s-long test pulses were applied to +40 mV every 60 s. Off-line leak subtraction and 3-point boxcar smoothing were used. Sampling and low-pass filter frequencies were 2000 and 1000 Hz, respectively.

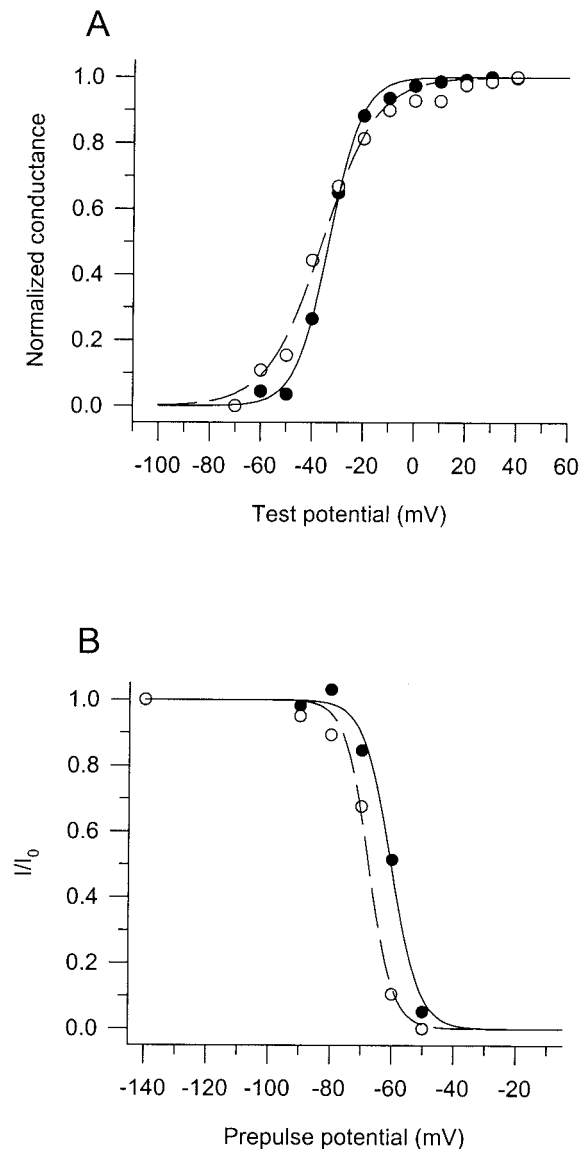


FIGURE 3 Effect of melatonin on the steady-state parameters of voltage-dependent gating of Kv1.3. (A) Voltage-dependence of steady-state activation of the K^+ current in a human T-lymphocyte in the presence and absence of melatonin. The cell was held at -120 mV holding potential and depolarized to the indicated test potentials for 40 ms every 50 s. Peak whole-cell conductance ($G(V)$) at each test potential was calculated from the peak current (I_p) at test potential V and the reversal potential (E_r). This latter quantity was determined independently from tail current experiments (see text). The $G(V)$ values were normalized for the maximum conductance and plotted (filled circles) as a function of test potential along with the best-fit Boltzmann function (normalized conductance = $1/(1 + \exp[(V - V_{1/2,a})/s_a])$), where V is the test potential, $V_{1/2,a}$ is the midpoint, and s_a is the slope of the function, (solid line). In control solution $V_{1/2,a} = -33.5$ mV and $s_a = -6.4$ mV were obtained for this cell. Continuous application of bath solution containing 2 mM melatonin changed the slope of the Boltzmann function ($s_a = -10.5$ mV) but caused a negligible shift in the midpoint ($V_{1/2,a} = -36.1$ mV). Normalized conductances in the presence of melatonin are shown with empty circles. (B) Voltage-dependence of steady-state inactivation of the K^+ current in a human T-lymphocyte in the presence and absence of melatonin. The applied prepulse-test pulse sequence was formed by a 150-s-long prepulse and a subsequent test pulse to $+50$ mV for 50 ms where the peak currents were measured. In every other

inactivation of Kv1.3, indicated by constant peak currents in the control solution. Switching to melatonin (1.5 mM) containing bath solution during the 60-s interpulse interval caused an instant reduction of the peak current in the first trace following the switch, and this reduction was constant for subsequent pulses in the presence of 1.5 mM melatonin, i.e., current reduction did not accumulate. Switching back to normal bath solution resulted in an instant recovery of the current.

Fifty-millisecond-long depolarization to $+40$ mV caused very little inactivation of Kv1.3. Thus we repeated the same pulse/perfusion protocol using 1-s-long depolarizations to $+40$ mV (Fig. 2 C), which inactivate $>95\%$ of Kv1.3 (Fig. 2 A). However, this did not change the pattern of current reduction (compare Fig. 2, B and C). Repeated pulses every 60 s gave constant peak currents before the application of the drug and current reduction did not accumulate from pulse to pulse in the continuous presence of melatonin. Moreover, there was no difference in the reduction of the current amplitude when using short (50-ms) or long (1000–2000-ms) depolarizing pulses at regular time intervals. The ratio of peak currents recorded in the presence and absence of 1.5 mM melatonin were 0.52 ± 0.02 and 0.50 ± 0.02 ($n = 16$ and 9 , $p = 0.28$) for short and long pulses, respectively (see also Fig. 2, B and C). Thus, reduction of the peak current was independent of the pulse protocol applied.

Reduction of the peak current in the presence of melatonin may be attributed to either an altered reversal potential of the current or to the reduction of the whole-cell K^+ conductance. To differentiate between these possibilities we determined the reversal potential of the current in the presence and absence of melatonin using standard tail current analysis (see below). Currents reversed at -82 ± 0.6 mV and -82.8 ± 1.5 mV in control solution and in the presence of 1.5 mM melatonin, respectively ($n = 3$, $p = 0.75$). Thus, current inhibition should be the consequence of a reduction in the whole-cell conductance in the presence of melatonin.

Both the voltage dependence of steady-state activation and inactivation were altered slightly by melatonin (Fig. 3,

prepulse-test pulse sequence the prepulse potential was set to -140 mV to avoid artifacts arising from gradual rundown of the current. The extent of steady-state inactivation was expressed as the ratio of peak currents recorded after a given prepulse potential (I) to the peak current preceded by -140 mV prepulse potential (I_0) in the previous pulse sequence. This ratio (I/I_0) is plotted as a function of prepulse potential for a T cell. Filled circles indicate points acquired in control external solution while hollow circles indicate those acquired in an external solution containing 1.5 mM melatonin. The midpoint of the Boltzmann function (see above) fitted to the points was shifted toward the negative potentials by melatonin ($V_{1/2,i} = -60.3$ mV for control and $V_{1/2,i} = -67.5$ mV in the presence of melatonin). At the same time the slope of the function was also slightly affected, $s_i = 4.5$ mV and $s_i = 4$ mV were obtained for control and in the presence of 1.5 mM melatonin, respectively.

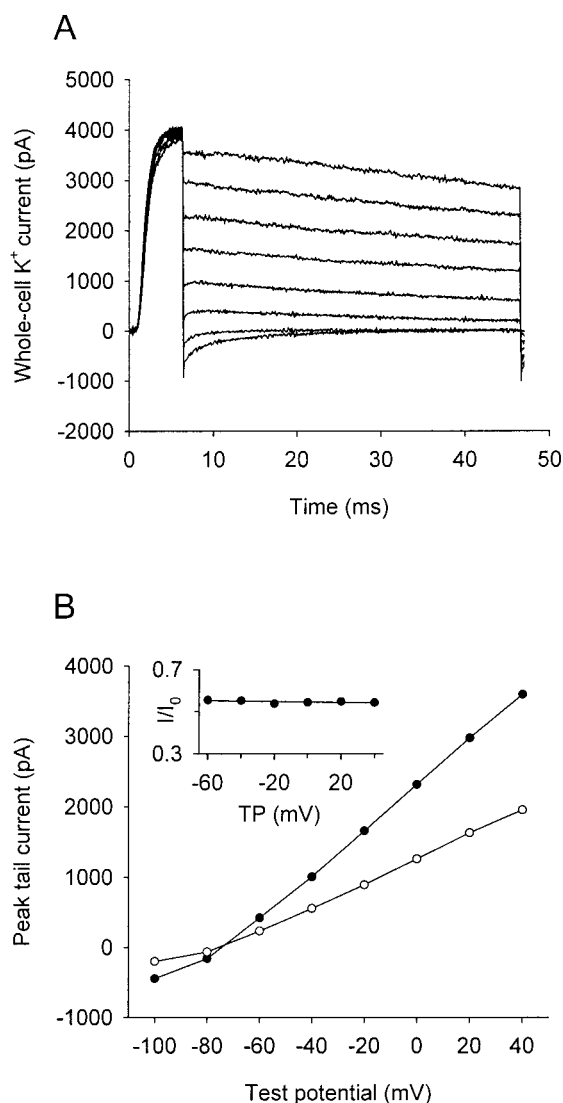


FIGURE 4 Voltage dependence of melatonin block studied by tail current analysis. (A) Tail currents of a human T cell. Channels were activated by a 5 ms pulse to +50 mV, then the voltage was stepped back to values ranging from -100 to $+40$ mV in 20-mV steps and tail currents were recorded. Pulses were separated by 60-s intervals at a holding potential of -120 mV. Sampling rate was changed from 50 to 16.6 kHz after the 5-ms pulse. Data were filtered at 5 kHz. P/7 leak subtraction was applied with subepisodes preceding the recorded sweep. (B) The effect of melatonin on the open channel current-voltage relationship. Instantaneous tail current amplitudes were determined at the indicated test potentials in the absence (filled circles) and in the presence (open circles) of melatonin (1.5 mM). The relationship was linear in both cases. *Inset*: Voltage dependence of melatonin block. The ratio of the peak tail current measured in the presence of 1.5 mM melatonin to that measured in control solution was calculated at each test potential in the -60 to $+40$ mV range. The average slope of the straight lines fitted to the data points was $-1.69 \times 10^{-4} \pm 9.1 \times 10^{-5} \text{ mV}^{-1}$.

A and B) as reported by the parameters of Boltzmann functions fitted to the normalized conductance versus test potential and remaining fraction of current (I/I_0) versus prepulse potential relationships, respectively (see figure leg-

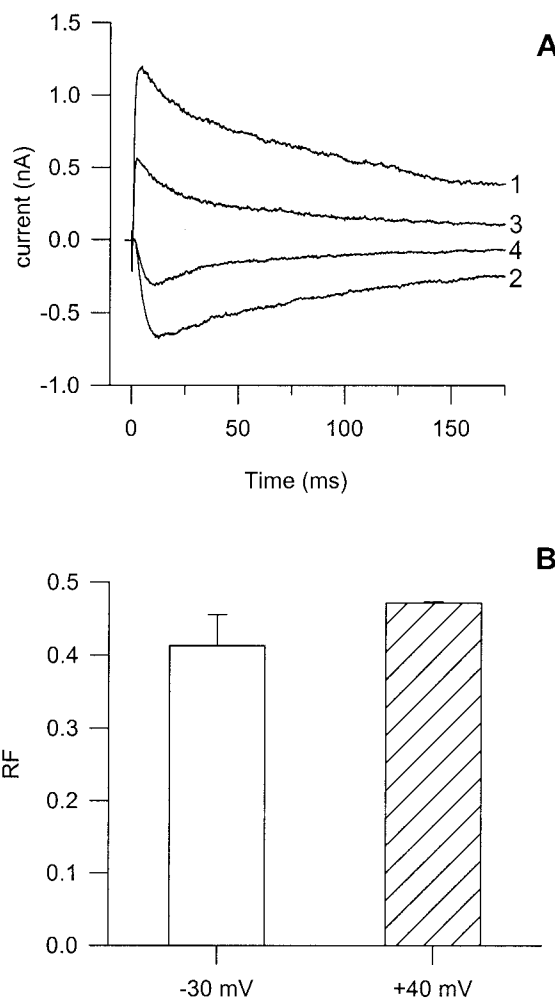


FIGURE 5 Block of inward and outward currents by melatonin. (A) A human peripheral blood T-lymphocyte was held at -120 mV and currents were recorded at depolarizations to either $+40$ (traces 1 and 3) or -30 mV (traces 2 and 4). These test potentials resulted in outward and inward currents, respectively, since the extracellular solution contained 150 mM K^+ . Traces 1 and 2 were recorded in drug-free solution, while current traces 3 and 4 were recorded in the presence of 1.5 mM melatonin. The sampling rate was 10 kHz, filter was set to 5 kHz. (B) The bars show the remaining fraction of current in the presence of 1.5 mM melatonin at test potentials -30 mV (open bar) and $+40$ mV (hatched bar). The remaining fraction of the current (I/I_0) was calculated as the ratio of peak currents in the presence (I) and absence (I_0) of melatonin (error bars indicate SE, $n = 3$).

ends for details). The midpoint of voltage dependence of steady-state activation ($V_{1/2,a}$) in control solution was -27.9 ± 1 mV. This value did not change significantly in the presence of 2 mM melatonin ($V_{1/2,a} = -28.1 \pm 3.2$ mV, $n = 5$, $p = 0.95$). The slope factor (s_a) however changed from $s_a = -9.6 \pm 0.7$ mV in control solution to $s_a = -15.7 \pm 2$ mV in the presence of 2 mM melatonin. The midpoint of voltage dependence of steady-state inactivation ($V_{1/2,i}$) was shifted by melatonin from $V_{1/2,i} = -58.3 \pm 1.8$ mV (control) to $V_{1/2,i} = -67.2 \pm 2.2$ mV (1.5 mM melatonin, $n = 5$, $p = 0.02$). This shift in the $V_{1/2,i}$ was not

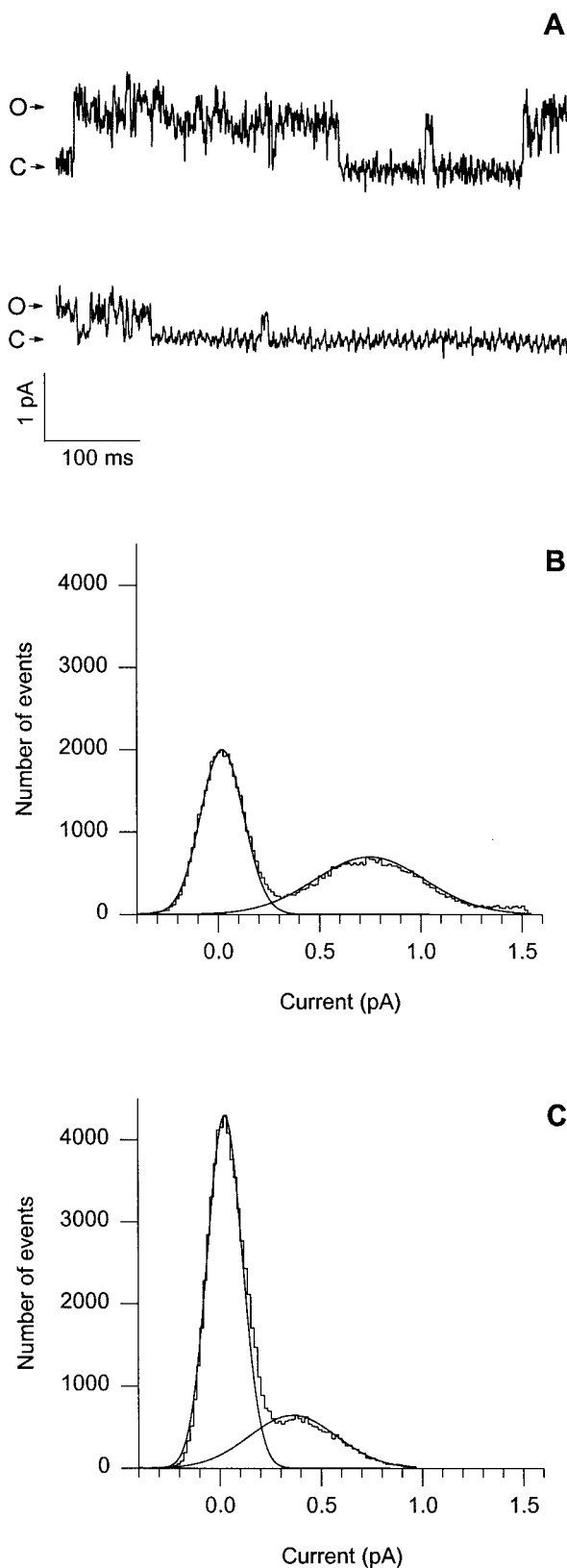


FIGURE 6 The effects of melatonin on single-channel currents of Kv1.3. (A) An outside-out patch was pulled from a human T-lymphocyte. Traces were recorded during depolarizing pulses to 0 mV from a holding

potential of -120 mV. Pulses were applied every 10 s and lasted for 1 s. Data were recorded at 5 kHz sampling rate and low-pass filtering was applied at 500 Hz. *Upper trace*: bath perfusion with control external solution. *Lower trace*: bath perfusion with external solution containing 5 mM melatonin. (B and C) All-points histograms were generated using 0.0157 pA bin-width. Superimposed continuous lines are the best fits to the histograms with the sum of two normal distributions. The fitted parameters in control solution (B) are $\mu_1 = 0.019$ pA, $\sigma_1 = 0.106$ pA, $\mu_2 = 0.748$ pA, $\sigma_2 = 0.272$ pA, where μ_n and σ_n are the mean and standard deviation of the n th component, respectively. The weight of the first component (non-conducting state) is 0.533. The fitted parameters in the presence of 5 mM melatonin are $\mu_1 = 0.026$ pA, $\sigma_1 = 0.086$ pA, $\mu_2 = 0.360$ pA, $\sigma_2 = 0.216$ pA. The weight of the first component is 0.746.

associated with a significant change in the slope factor (control: $s_i = 4.1 \pm 0.7$; melatonin: $s_i = 5.1 \pm 0.6$ mV, $n = 5$, $p = 0.11$). Regardless of the change in $V_{1/2,i}$ and s_a , the voltage dependence of normalized activation and steady-state inactivation functions of control and melatonin-treated cells assume the same values at holding potentials more negative than -120 mV and test potentials more positive than $+40$ mV. Thus, melatonin-induced changes in s_a and $V_{1/2,i}$ set a membrane potential window for voltage protocols where reduction of the peak currents is attributed to the *block of potassium channels* by the drug. Accordingly, this voltage range was used in this study (including data shown previously in Fig. 2).

To determine whether the change in s_a is due to voltage-dependent block by melatonin we measured the open channel current-voltage relationship with or without melatonin in the bath solution. Because block equilibration is very fast (see below in Fig. 6) instantaneous tail currents at each potential should represent the fraction of the channels not blocked by melatonin.

Fig. 4 shows the recorded tail currents (A) and the instantaneous current voltage relationship in the absence and presence of 1.5 mM melatonin (B). Some rectification was observable below -60 mV for both cases, but at potentials more positive than -60 mV the current-voltage relationships were perfectly linear with $r^2 = 0.999 \pm 0.0003$ and 0.997 ± 0.0010 for control and after melatonin treatment (1.5 mM), respectively ($n = 5$). The ratios of instantaneous tail current amplitudes measured with 1.5 mM melatonin in the bath to those measured in control extracellular solution were calculated and plotted as a function of test potential (inset to Fig. 4 B) to investigate the voltage dependence of melatonin block. Straight lines were fitted to the points yielding an average slope and intercept of $-1.69 \times 10^{-4} \pm 9.1 \times 10^{-5}$ mV $^{-1}$ and 0.52 ± 0.01 ($n = 5$), respectively. The negligible slope implies a lack of voltage dependence of melatonin block.

Moreover, the degree of block was independent of the direction of current flow. Fig. 5 shows currents recorded in symmetrical K^+ (150 mM) solution in the presence and

potential of -120 mV. Pulses were applied every 10 s and lasted for 1 s. Data were recorded at 5 kHz sampling rate and low-pass filtering was applied at 500 Hz. *Upper trace*: bath perfusion with control external solution. *Lower trace*: bath perfusion with external solution containing 5 mM melatonin. (B and C) All-points histograms were generated using 0.0157 pA bin-width. Superimposed continuous lines are the best fits to the histograms with the sum of two normal distributions. The fitted parameters in control solution (B) are $\mu_1 = 0.019$ pA, $\sigma_1 = 0.106$ pA, $\mu_2 = 0.748$ pA, $\sigma_2 = 0.272$ pA, where μ_n and σ_n are the mean and standard deviation of the n th component, respectively. The weight of the first component (non-conducting state) is 0.533. The fitted parameters in the presence of 5 mM melatonin are $\mu_1 = 0.026$ pA, $\sigma_1 = 0.086$ pA, $\mu_2 = 0.360$ pA, $\sigma_2 = 0.216$ pA. The weight of the first component is 0.746.

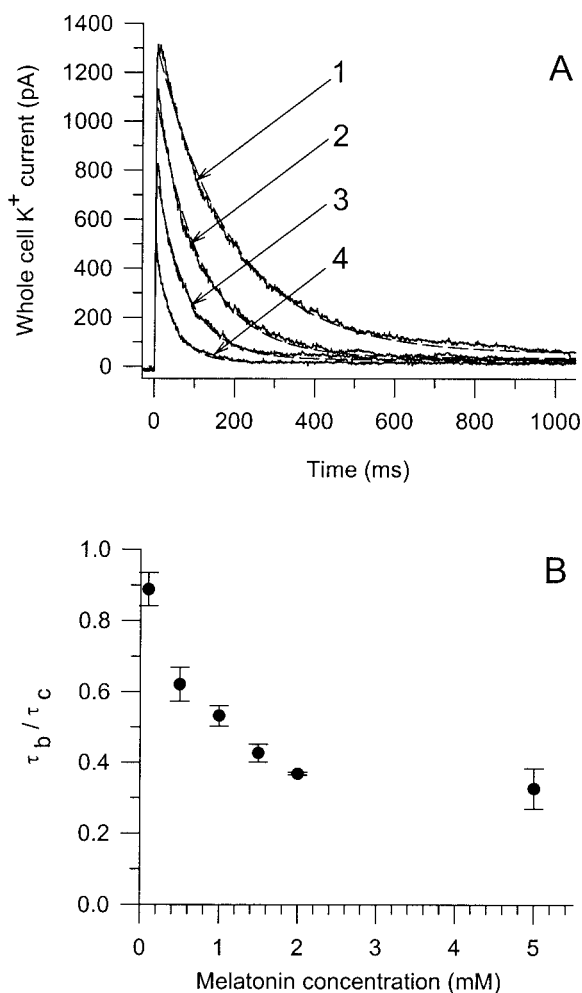


FIGURE 7 Inactivation of the K^+ current in the presence of melatonin. (A) Whole-cell K^+ currents of a human peripheral T lymphocyte recorded during 2-s-long test pulses to +40 mV from a holding potential of -120 mV. Test pulses were applied every 90 s. The bath was perfused with control solution (1), a solution containing 0.5 mM (2), 1.0 mM (3), and 2.0 mM melatonin. During the experiment excess fluid was removed by continuous suction. Sampling and low-pass filter frequencies were 1000 and 500 Hz, respectively. Superimposed dashed lines are the best-fit single exponential functions to the decay of the currents: $I(t) = A \times \exp(-t/\tau) + C$, where A and C are the amplitudes of the inactivating and noninactivating components, respectively, and τ is the time constant. The values of τ were 189.3 ms (1), 114.0 ms (2), 76.3 ms (3), and 45.2 ms (4). (B) The ratio of inactivation time constants of whole-cell K^+ currents in the presence (τ_b) and absence (τ_c) of melatonin were plotted as function of melatonin concentration. Error bars indicate SE ($n = 2-4$).

absence of melatonin. At -30 and $+40$ mV test potentials the currents are inward and outward, respectively (Fig. 5 A). The ratios of peak currents measured in the presence and absence of melatonin at different membrane potentials are shown in Fig. 5 B. The remaining fraction of the current in the presence of 1.5 mM melatonin was the same regardless of the direction of current flow ($n = 3$, $p = 0.31$, paired t -test).

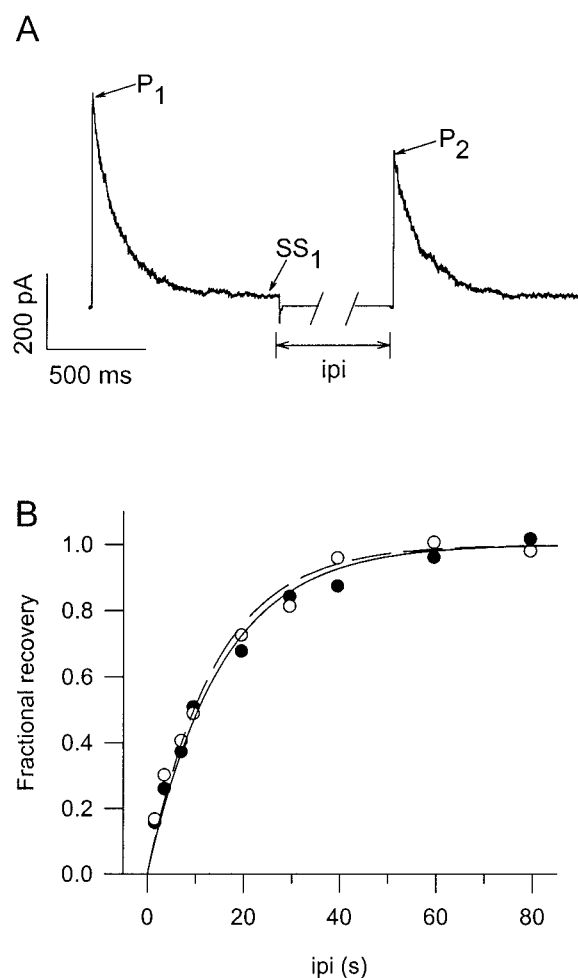


FIGURE 8 Recovery from inactivation is not changed by melatonin. (A) A human T-lymphocyte in whole-cell clamp was held at -120 mV and a pair of test pulses (1 s duration) to +40 mV was applied separated by a 6.5-s interpulse interval (ipi). The peak currents during the first pulse (P_1), during the second pulse (P_2), and the current at the end of the first pulse (SS_1) were measured. From these data fractional recovery was calculated as in the text. The membrane was held at -120 mV during the ipi . Sampling frequency was 1 kHz. (B) Fractional recovery of potassium current as a function of ipi in control extracellular solution (filled circles) and in an external solution containing 2 mM melatonin (open circles). Points were fitted with a single rising exponential function (see text). The solid and dashed lines represent the best fit to the data obtained in control conditions and in the presence of melatonin, respectively. The corresponding time constants for recovery from inactivation were 15.2 s and 13.9 s for control and in the presence of melatonin, respectively.

Single-channel amplitude is reduced by melatonin

Fig. 6 shows single-channel currents recorded from an outside-out-patch in the absence and presence of melatonin. The all-points histogram generated from the trace recorded at 0 mV in normal bath solution peaks at $\mu = 0.75$ pA ($\sigma = 0.27$ pA) corresponding to 9.1 pS conductance, in agreement with the literature (Lee et al., 1992). Extracellular

addition of melatonin decreased the amplitude of single-channel currents (Fig. 6 C). Average current amplitude was reduced to $77.7 \pm 0.5\%$ of the control by 1.5 mM and to $58.3 \pm 6.3\%$ by 5 mM melatonin. Our interpretation of the reduction in the average amplitude is that the transition between the conducting (no melatonin bound) and the non-conducting (melatonin bound) states is very fast so that blocked periods are too brief to be resolvable using our recording apparatus. Instead, an average of the currents from the open and blocked periods is recorded, similarly to the block of *Shaker* K^+ channels by TEA (Spruce et al., 1987). In this case both the on and off rates of the drug must be fast as it is illustrated in Fig. 2, B and C.

Effect of melatonin on the inactivation properties of Kv1.3 current

Fig. 2 A shows that besides blocking the potassium current melatonin also increases the rate of current inactivation. We studied the dose dependence of this effect. The kinetics of inactivation of the whole-cell Kv1.3 current was characterized by the time constant of a single-exponential function fitted to the data points. In control solution the resulting time constant was $\tau_c = 188 \pm 7$ ms ($n = 7$) determined at +40 mV test potential. At all melatonin concentrations the current decay could well be fitted with a single-exponential function (Fig. 7 A, see legend). Fig. 7 B shows that increasing concentrations of melatonin sped inactivation in a dose-dependent manner, manifesting in a decreased ratio of τ_b/τ_c with increasing drug concentration, where τ_b and τ_c are the inactivation time constants in the presence and absence of the drug, respectively.

Fig. 7 suggests that the concentration-dependent increase in current inactivation is the result of faster inactivation of melatonin-bound channels. Inactivated channels with bound melatonin might recover at different rates from inactivation as compared to control, thereby indicating the binding of melatonin to the inactivated channels. This was tested in the experiments described below.

The kinetics of recovery from inactivation was measured by a conventional protocol using pulse pairs (Fig. 8 A). One pulse pair consisted of 1-s-long test pulses (+40 mV) separated by various interpulse intervals (*ipi*) ranging from 1 to 80 s at -120 mV. The 1-s-long test pulse was enough to inactivate $>95\%$ of the current. Time between pulse pairs was 120 s at a holding potential of -120 mV to allow full recovery of the channels. The fraction of channels recovered (*FR*) from the inactivated state at any *ipi* was calculated using the following formula: $FR = (P_2 - SS_1)/(P_1 - SS_1)$, where P_1 and P_2 are peak currents detected during the first and the second pulses in the pair, respectively, and SS_1 is the amplitude of the current at the end of the first pulse. *FR* calculated using this formula is free from contamination by any nonspecific conductance, as well as different levels of current at the end of the first depolarization. We determined

the time constant for recovery from inactivation by plotting *FR* as the function of interpulse interval and fitting a single-exponential function: $FR(ipi) = 1 - \exp(-ipi/\tau)$ to the data points (Fig. 8 B). The time constants for recovery from inactivation were 11.2 ± 2.1 s and 11.0 ± 2.1 s for control and in the presence of 2 mM melatonin, respectively. The difference was not statistically significant ($n = 3$, $p = 0.82$, paired *t*-test).

Peak currents represent equilibrium block of potassium current

Fig. 2, B and C show that reduction of the peak current is instantaneous after the start of the perfusion regardless of the pulse protocol applied. However, these experiments did not exclude the possibility of slow equilibration of the block in the closed state of the channel. This possibility was tested in the next experiment (Fig. 9). We compared the percentage of current block in cases when depolarizing pulses were regularly applied following the start of the application of melatonin (first application of melatonin in Fig. 9, protocol A) with those in which channels were kept closed for several minutes during the application of melatonin and then depolarized to measure the current (second application of melatonin in Fig. 9, protocol B). The reduction in the peak currents was essentially the same, 50% and 47%, calculated from protocols A and B, respectively.

In summary, the above experiments shown in Figs. 2–9 support the idea that a use-dependent block can be excluded and that the reduction of the peak currents reflects equilib-

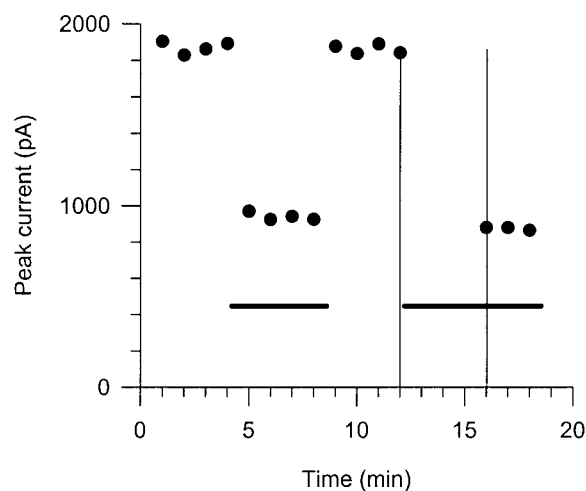
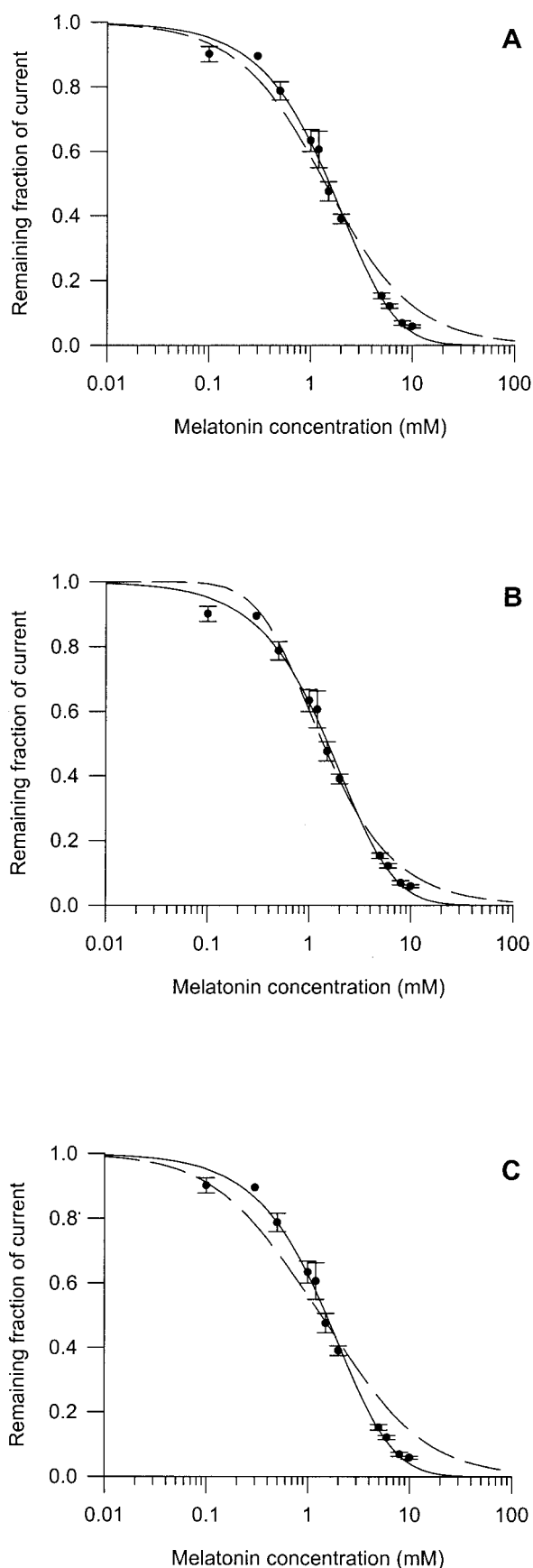


FIGURE 9 Closed-state association of melatonin to Kv1.3. Whole-cell peak currents recorded in a human T lymphocyte during test pulses to +40 mV from a holding potential of -120 mV. Horizontal bars indicate the duration of bath perfusion with a solution containing 1.5 mM melatonin. Test pulses were applied every 60 s except the gap between 12 and 16 min (between vertical lines) where 1.5 mM melatonin was already applied but test pulses were suspended. Pulse duration was 50 ms, sampling frequency 20 kHz.



rium block of the channels under the applied conditions. A possible explanation for the reduced peak currents in the presence of melatonin is that it binds to the closed state of the channels and remains bound once the channels open. Alternatively, it binds to the open state at much higher rates that can be resolved in patch-clamp experiments, similarly to the action of TEA. Furthermore, the increased inactivation rate of the current can be a consequence of modulation of inactivation by binding of melatonin.

Four available binding sites for melatonin

The blocking effect of melatonin was dose-dependent, with a half-blocking concentration of 1.5 mM. A theoretical curve based on 1:1 channel/melatonin stoichiometry (model I) gave a poor fit to the measured points at various concentrations (Fig. 10 A), thus we looked for alternative models. Because Kv1.3 channels are made up of four identical subunits, the assumption that four independent melatonin binding sites exist on each channel seemed logical.

Even in this case several alternatives had to be considered. First, a single melatonin molecule binding to any of the four sites is sufficient to block the channel (model IIa). Second, all four sites must be occupied by melatonin to block the channel, but unitary conductance is not affected when only one, two, or three molecules are bound (model IIb). Third, each melatonin molecule binding to a site on the channel decreases the single-channel conductance in a step-wise fashion (model IIc).

The probability that a melatonin molecule binds to an individual binding site (1:1 stoichiometry) at melatonin concentration $[m]$ is $p = [m]/([m] + K_d)$, where K_d is the dissociation constant, i.e., the melatonin concentration at which half of the binding sites are occupied (Hille, 1992). Accordingly, the probability that no melatonin molecule binds to it is $q = 1 - p = K_d/([m] + K_d)$.

Dose-response functions for the three different models can be constructed using the binomial distribution (Mac-

FIGURE 10 Comparison of the various models of melatonin binding. Peak whole-cell currents in human T-lymphocytes were measured at depolarizing test pulses to +40 mV from a holding potential of -120 mV. The unblocked fraction of the peak current was calculated at different melatonin concentrations as I/I_0 , where I_0 and I were the peak currents measured in the control solution and in solutions containing different concentrations of melatonin, respectively. On each panel the measured points and the SE ($n = 3-11$) are displayed with two fitted functions corresponding to different models. The solid line on each panel represents the model in which the binding of one melatonin molecule to any of the four binding sites on the channel is enough to block the channel (model IIa). The dashed lines represent the other models: (A) one binding site per channel, one bound molecule blocks the channel (model I); (B) four binding sites per channel, all four must be occupied to block the channel (model IIb); (C) four binding sites per channel, each molecule binding to the channel decreases the unitary current amplitude by one-fourth of the original amplitude (model IIc).

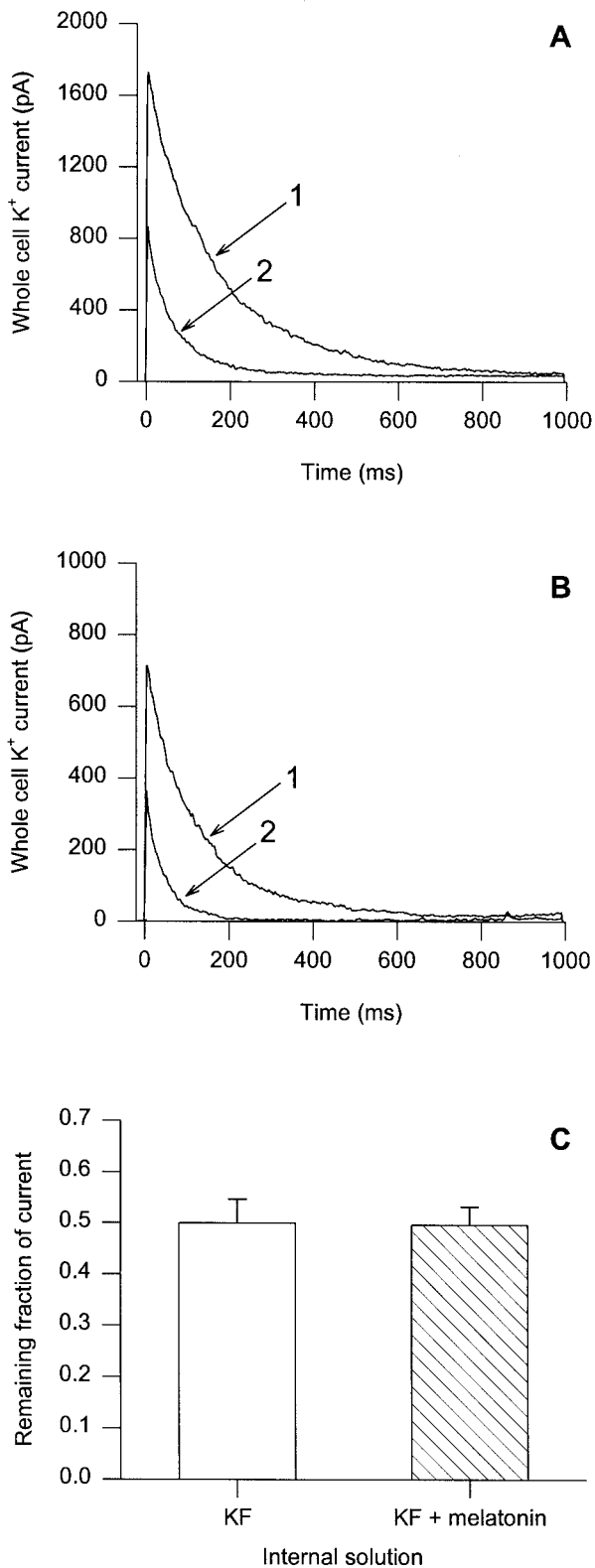


FIGURE 11 Simultaneous application of melatonin from the intracellular and extracellular sides. Whole-cell K⁺ currents of human T-lymphocytes are displayed (1) before and (2) after the extracellular application of 1.5 mM melatonin using (A) control internal solution and (B) internal solution containing 1.5 mM melatonin. Other experimental conditions were

Kinnon, 1991). In this case the probability that of the $n = 4$ independent sites exactly k are occupied by melatonin molecules is

$$P_k = \frac{n!}{k!(n-k)!} p^k q^{n-k} \quad (1)$$

If a single melatonin molecule is sufficient to block the channel, then the channel conducts only if none of the sites is occupied. The probability of this event is $q^4 = [K_d/([m] + K_d)]^4$, which gives the remaining fraction of the current at melatonin concentration $[m]$ in a whole-cell measurement. However, if all four sites must be occupied for the block to occur, then the fraction of unblocked channels is $1 - p^4 = 1 - [[m]/([m] + K_d)]^4$.

The theoretical functions derived from the various models are compared in Fig. 10. The best fit to the experimental data was obtained with model IIa, therefore this model (solid line) is presented in comparison with each of the other models (dashed line) on panels A–C. In Fig. 10 A the 1:1-binding site to channel stoichiometry is compared with model IIa. In Fig. 10 B both models assume four binding sites per channel, but in one of the models one melatonin molecule is enough to block the channel (IIa), in the other four molecules are required to do so (IIb). K_d values for individual binding sites obtained from the fits were 8.11 mM and 0.26 mM for models IIa and IIb, respectively.

The simplest function representing model IIc is based on the assumption that each melatonin molecule that binds to the channel decreases the current amplitude by one-fourth of the original amplitude. Thus, the current amplitude is reduced to 0.75, 0.5, or 0.25 times of the maximum amplitude when one, two, or three melatonin molecules are bound to the channel, respectively, and four bound molecules are required to block the channel completely. In this case the whole-cell current is given by the binomially weighted sum of five terms:

$$\frac{I}{I_0} = \sum_{k=0}^4 P_k \frac{4-k}{4}, \quad (2)$$

where k is the number of binding sites per channel occupied by melatonin. The K_d value for the individual binding sites is 1.72 mM for this model. The fitted function based on this

the same as for Fig. 2. (C) Remaining fraction of current was calculated as I/I_0 , where I_0 is the peak of the current recorded with no melatonin in the bath and I is the peak during the extracellular application of 1.5 mM melatonin. The open and hatched bars show the remaining fraction of current recorded with normal and melatonin (1.5 mM) supplemented pipette filling solutions, respectively. Extracellular application of 1.5 mM melatonin resulted in the same fractional decrease in current amplitude when the pipette solution contained 1.5 mM melatonin or was melatonin-free ($p = 0.95$).

model is also compared with model IIa in Fig. 10 C and clearly gives a worse fit to the measured data.

The comparison of the dose-response functions based on their goodness of fit reveals that the model that best describes the experimental observations is the one in which the binding of a single melatonin molecule to any of the four binding sites on the channel blocks the channel (model IIa). The goodness of fit was assessed by calculating the residual sum of squares for each curve. In principle, the model with the lowest residual sum of squares gives the best fit if the number of degrees of freedom (i.e., number of data points minus the number of parameters) is the same for all models. In our case this condition was fulfilled since the number of data points was constant and each fitted function had one free parameter, K_d (Motulsky and Ransnas, 1987). The residual sum of squares were 0.036, 0.006, 0.021, and 0.07 for models I through IIc, respectively.

Melatonin acts from the extracellular side

Several effects of melatonin can be attributed to its ability to cross biological membranes (Costa et al., 1995). Therefore we wanted to determine whether it binds to Kv1.3 from the intracellular or extracellular side. The fact that both extracellular blocking and washout occur very quickly suggests that melatonin binds directly from this side. We tested this hypothesis by introducing melatonin to the pipette solution and assessing the block of potassium current by extracellular melatonin applied in the same concentration (1.5 mM) as in the pipette solution. This way, if melatonin were to act from the inside it would block the appropriate fraction of channels, and the extracellularly applied melatonin should have no further effect on the current. However, if melatonin acts from the outside extracellular melatonin should affect the current the same way it would when using regular pipette solution. The results of these experiments are summarized in Fig. 11. The results show no significant differences in the reduction of current amplitudes between measurements with or without intracellular melatonin. Thus, these results prove that melatonin block occurs from the extracellular side of the membrane.

Simultaneous occupancy of binding sites by melatonin and ChTx

ChTx blocks potassium channels by simply occluding the pore. Binding of ChTx and another pore blocker, TEA, to the pore of voltage- and calcium-activated potassium channels is mutually exclusive, indicating overlapping binding sites for ChTx and TEA (Miller, 1988; Goldstein and Miller, 1993). Similarly, we examined the relationship of ChTx and melatonin binding to Kv1.3. The protocol applied is shown in Fig. 12 A. The remaining fractions of whole-cell peak currents were determined in the presence of melatonin,

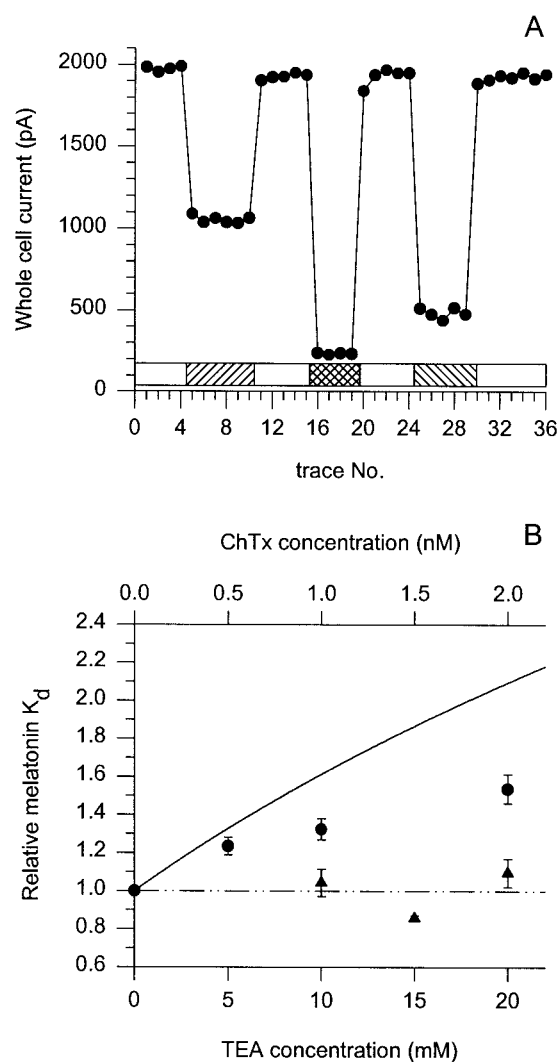


FIGURE 12 Effects of TEA and ChTx on melatonin binding to Kv1.3 channels. (A) Peak whole-cell currents in a human peripheral blood T-lymphocyte are plotted as a function of trace number in a series of identical depolarizations. The cell was held at -120 mV for 50 s between depolarizing pulses to $+40$ mV lasting for 50 ms. The solutions used for the perfusion of the external bath are indicated by the bar on the lower part of the figure: control solution (empty bar), 1.5 mM melatonin (left-hatched), simultaneous presence of 1.5 mM melatonin and 1.5 nM ChTx (cross-hatched), and 1.5 nM ChTx (right-hatched). The remaining fractions of currents determined from this experiment were $RF_m = 0.533$, $RF_s = 0.122$, $RF_{ChTx} = 0.25$, and $RF_m|ChTx = 0.488$. (B) Comparison of competition models. The binding affinity of melatonin was studied at various concentrations of TEA (bottom x axis) and ChTx (top x axis). The dash-dot-dot line represents the model in which melatonin and the other blocker bind independently leaving, the K_d of melatonin unaffected (see text for details). The solid line represents the competition model in which melatonin and the other blocker cannot be present on the same channel simultaneously. Each data point represents the mean \pm SE ($n = 3-4$) of the relative dissociation constants calculated from the measured data at the indicated TEA (circles) and ChTx concentrations (triangles). Relative K_d was calculated as the ratio of apparent K_d of melatonin in the presence of TEA or ChTx and its real K_d in the absence of TEA and ChTx. Apparent K_d was determined from $RF_m|ChTx$ and $RF_m|TEA$ (see text for details) based on model IIa. The binding affinity of melatonin to wild-type channels is influenced by TEA (circles) but not by ChTx (triangles).

in the presence of ChTx, and during simultaneous administration of the two compounds.

The remaining fraction of the whole-cell current in the simultaneous presence of both ChTx and melatonin can be written as $RF_s = 1 - [P(\text{ChTx}) + P(\text{m}) - P(\text{ChTx} + \text{m})]$, where $P(\text{ChTx})$ is the probability of ChTx block, $P(\text{m})$ is the probability of melatonin block, and $P(\text{ChTx} + \text{m})$ is the probability that both compounds are bound to the channel simultaneously. If the binding of one has no effect on the binding of the other, then $P(\text{ChTx} + \text{m}) = P(\text{ChTx}) \times P(\text{m})$, since the probability of independent events occurring simultaneously is the product of their individual probabilities. In the absence of ChTx the application of melatonin would result in a remaining current fraction of $RF_m = 1 - P(\text{m})$. If both ChTx and melatonin are present and the current in the presence of ChTx alone (RF_{ChTx}) is taken as control, the remaining fraction of the current would be $RF_m|\text{ChTx} = RF_s/RF_{\text{ChTx}} = (1 - [P(\text{ChTx}) + P(\text{m}) - P(\text{ChTx}) \times P(\text{m})]) / (1 - P(\text{ChTx}))$. Comparison of the expressions for RF_m and $RF_m|\text{ChTx}$ reveals that the extent of current reduction by melatonin would not depend on whether ChTx is present. Therefore, the apparent K_d value for melatonin calculated from $RF_m|\text{ChTx}$ would be constant at all ChTx concentrations and equal to its real K_d value, calculated from RF_m . This model is represented on Fig. 12 B by the dash-dot-dot line.

By using 1.5 mM melatonin concentration and increasing concentrations of ChTx, apparent K_d values were determined experimentally, and the ratio of the apparent and real K_d values was plotted on the graph as a function of ChTx concentration. The data points are scattered around the dash-dot-dot line, indicating independent binding of melatonin and ChTx to the channel. This indicates that the binding sites for these two molecules are not overlapping, melatonin and ChTx can bind simultaneously to the channel.

Melatonin interacts with TEA binding to Kv1.3

Melatonin speeds C-type inactivation of Kv1.3 (see Figs. 2 A and 7). Inactivation kinetics of *Shaker* potassium channels is very sensitive to the nature of amino acid side chains and their physical state at position 399 (López-Barneo et al., 1993). Amino acids at the same position are responsible for creating a binding site for extracellular TEA (Heginbotham and MacKinnon, 1992; Kavanaugh et al., 1991). We have monitored this region of the channel through the TEA binding site by characterizing the interaction of melatonin and TEA binding to their respective receptors.

By using the same experimental protocol as for the previous section, we have expressed the apparent K_d value for melatonin from $RF_m|\text{TEA} = RF_s/RF_{\text{TEA}}$, where RF_s is the remaining fraction of current in the simultaneous presence of TEA and melatonin, and RF_{TEA} is the remaining fraction of current in the presence of TEA only. The ratio of the apparent K_d , calculated from $RF_m|\text{TEA}$, over the real K_d ,

calculated from RF_m (see above), is plotted as a function of TEA concentration in Fig. 12 B. The data points are all above the horizontal dash-dot-dot line corresponding to the independent binding of the two compounds. This means that melatonin and TEA do not bind independently to Kv1.3. The data points are also far below the solid line representing the competition between melatonin and TEA for the same binding site. The model describing competition of melatonin and TEA (*solid line*) for the same binding site (mutually exclusive binding) was constructed as follows.

Assuming that the occupancy of one of the four binding sites of melatonin is sufficient to prevent TEA from binding, the remaining fraction (RF_s) of the whole-cell current in the simultaneous presence of melatonin and TEA at concentrations $[\text{m}]$ and $[\text{TEA}]$, respectively, is given by

$$RF_s = \frac{1}{[\text{TEA}]/K_d^{\text{TEA}} + (1 + [\text{m}]/K_d^{\text{m}})^4} \quad (3)$$

where $K_d^{\text{TEA}} = 11.1$ mM and $K_d^{\text{m}} = 8.11$ mM were determined experimentally (see details of the model calculations in the Appendix). Taking the current in the presence of TEA alone as 100% and solving the equation for $[\text{m}]$, the melatonin concentration that reduces the current amplitude by 50% at any TEA concentration can be calculated. From this half-blocking melatonin concentration an apparent K_d value for the mutually exclusive binding model can be calculated, which will be greater than the actual 8.11 mM. The ratio of this apparent K_d value, calculated from the model, and the real K_d value is plotted on the graph as a function of TEA concentration. This is represented in Fig. 12 B by the solid line.

Data points acquired in the simultaneous presence of TEA and melatonin fall between the two lines representing the different models described above. This means that TEA reduces the affinity of the melatonin binding site for its ligand in a concentration-dependent manner ($p = 0.02$, ANOVA). From the same set of data the effect of melatonin on the TEA binding site was determined. Based on 1:1 stoichiometry of TEA binding to its receptor site, the K_d value of TEA was calculated from the remaining fraction of current in the presence of TEA only ($K_d = 11.1 \pm 0.4$ mM, $n = 10$). Similarly, from $RF_{\text{TEA}}|\text{m} = RF_s/RF_m$, where RF_s is defined above and RF_m is the remaining fraction of current in the presence of melatonin only, the apparent K_d value for TEA was calculated. At constant 1.5 mM melatonin concentration the apparent K_d values for 5, 10, and 20 mM TEA were 18.8 ± 2.9 mM ($n = 4$), 16.5 ± 1.2 mM ($n = 3$), and 16.6 ± 0.3 mM ($n = 3$), respectively. The apparent K_d over real K_d ratios at different TEA concentrations were constant ($p = 0.595$, ANOVA), and the pooled average was 1.53 ± 0.09 ($n = 10$). This means that melatonin significantly reduced the affinity of the TEA binding site for its ligand ($p < 0.001$).

In summary, TEA and melatonin mutually modify the affinity of the receptor sites for their respective ligands. This interaction is allosteric modification because melatonin and TEA bind to different receptors: they do not compete for the same (or overlapping) binding site.

The block of slowly inactivating mutant (H399Y) channels by melatonin

To get a deeper insight into the modulation of inactivation and the state dependence of melatonin block we studied the effect of melatonin on a Kv1.3 mutant (H399Y), which inactivates very slowly (Fig. 13 A). Position 399 corresponds to T449 in *Shaker* channels. This position is a major determinant of drug binding to the extracellular mouth of *Shaker* potassium channels (Kavanaugh et al., 1991; Heginbotham and MacKinnon, 1992). Accordingly, binding affinity for TEA is enhanced ~ 40 -fold by the H399Y mutation (Panyi and Deutsch, 1997). At the same time amino acid side chains in this position influence dramatically the rate of C-type inactivation (López-Barneo et al., 1993). Fig. 13 A shows K^+ currents recorded in CTLL-2 cells expressing the H399Y mutant channels. The current inactivated much slower than the wild-type Kv1.3 current shown in Fig. 2. The decay of the current was not monoexponential as for the wild-type current, but the 5.4-s segments of the current traces shown in Fig. 13 A were well fitted by the sum of two exponential terms. Fitting longer sections of the 23.6-s-long test pulses using the sum of two terms resulted in poor fits and large scatter in the fitted parameters (not shown). This is most probably the consequence of a more complex inactivation of this mutant requiring more than two inactivated states for correct fits. However, the first 5.4-s segment of the traces included much of the decay and provided reliable fitted parameters. The fast and the slow components of the decay had time constants of $\tau_f = 253.8 \text{ ms} \pm 17.9 \text{ ms}$ and $\tau_s = 1766.5 \pm 70.9 \text{ ms}$, respectively ($n = 4$). The corresponding (normalized) preexponential terms were 0.40 ± 0.08 and 0.37 ± 0.04 for the fast and the slow components, respectively.

Melatonin also blocks H399Y channels (*trace 2* in Fig. 13 A). The dose-response curve of melatonin for H399Y channels was created using the same approach as described for Fig. 10. Peak currents were measured during test pulses to +40 mV from a holding potential of -120 mV in control solution and at different concentrations of melatonin in the bath. Fig. 13 B shows the remaining fraction of current at different melatonin concentrations for cells expressing H399Y channels along with data from Fig. 10 obtained for Kv1.3 in peripheral blood lymphocytes. The data points and fitted dose response curves using model IIa are practically identical. The fitted K_d value of melatonin for the H399Y channels is 8.4 mM, which is very close to 8.11 mM determined for Kv1.3. This means that the dramatic slowing

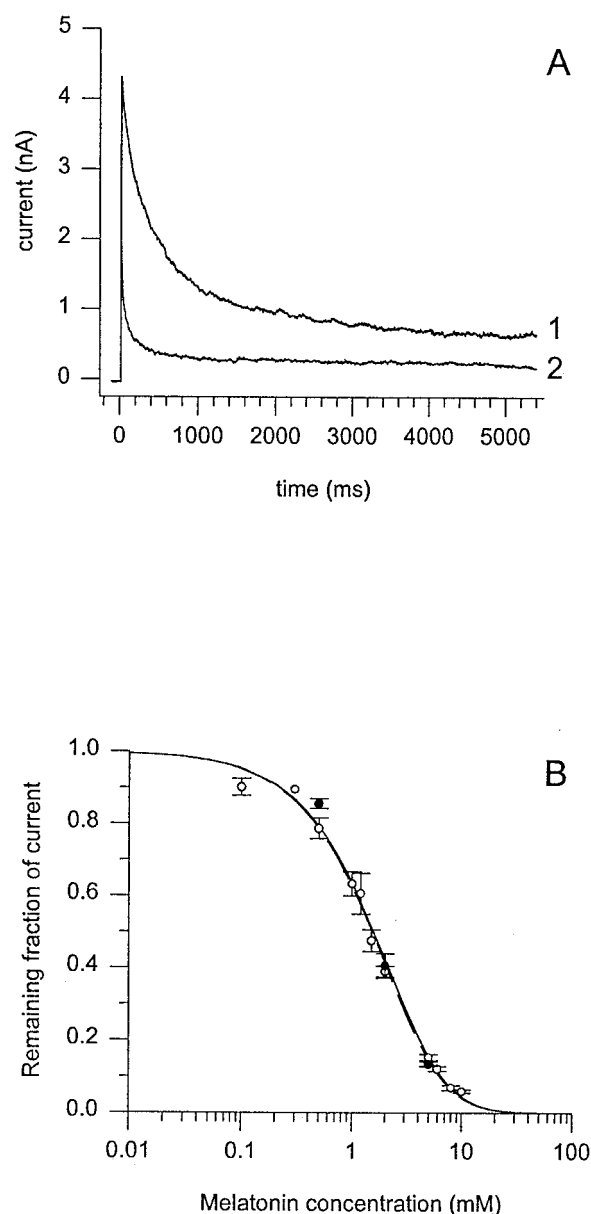


FIGURE 13 Melatonin affinity is unaffected by the H399Y mutation. (A) A CTLL-2 cell expressing Kv1.3 H399Y mutant gene displayed whole-cell outward currents when the membrane potential was changed from a holding potential of -120 mV to $+40 \text{ mV}$. A 5.4-s-long segment of 23.6-s-long depolarization is shown before (*trace 1*) and after the application of 1.5 mM melatonin (*trace 2*). Sampling frequency was 666 Hz . (B) The unblocked fraction of the peak current (I/I_0) was calculated and plotted at different melatonin concentrations. I_0 and I are the peak currents measured in the control solution and in solutions containing different concentrations of melatonin, respectively, at $+40 \text{ mV}$ test potential (holding potential = -120 mV). Hollow circles indicate points measured on wild-type Kv1.3 channels in human T cells, filled circles represent points measured on H399Y mutant channels in CTLL-2 cells. Error bars indicate SE ($n = 3-11$). The dashed line is the binding curve fitted to the data points measured on wild-type channels based on a 4:1 drug/channel stoichiometry, when one bound melatonin molecule is sufficient to block the channel. The solid line is the curve fitted to the points measured on mutant channels based on the same model.

of the inactivation gating of H399Y channels has no consequence on melatonin binding.

In the presence of melatonin the inactivation rate of the H399Y current was increased (Fig. 13 A). The characteristic values of the decay in the presence of 1.5 mM melatonin became $\tau_f = 51.6 \pm 12.8$ s and $\tau_s = 511 \pm 145.7$ ms ($n = 4$). The normalized preexponential terms became 0.52 ± 0.02 and 0.30 ± 0.12 for the fast and slow components, respectively, so both the decreased time constants and the increased weight of the faster component are responsible for the faster kinetics of inactivation in the presence of melatonin.

DISCUSSION

Human peripheral blood T-lymphocytes express a variety of ion channels (Cahalan and Lewis, 1990) among which the most abundant types are voltage-gated (Kv1.3) and Ca^{2+} -activated potassium channels (Matteson and Deutsch, 1984; Cahalan et al., 1985; Grissmer et al., 1993). The relative weight of these channels over other channel types was increased by mitogen stimulation of T cells by PHA (Levy and Deutsch, 1996; Grissmer et al., 1993). At the same time, the pipette filling solution used in this study contained 140 mM KF and 11 mM EGTA providing free Ca^{2+} concentration in the low nM range, thereby excluding the contribution of Ca^{2+} activated K^+ channels to the whole-cell current (Grissmer et al., 1993). Therefore, the contamination of whole-cell currents by channels other than Kv1.3 was negligible. Thus, the block of Kv1.3 channels by melatonin was studied in this paper.

We found that melatonin reduced the whole-cell K^+ current of PHA-activated human T cells in a dose-dependent manner. The following lines of evidence support that melatonin blocks Kv1.3 channels: 1) the effect of melatonin is reversible (Fig. 2 A); 2) the reversal potential of the current was not changed by melatonin; 3) the normalized voltage-dependence of steady-state activation (Fig. 3 A) and inactivation (Fig. 3 B) curves recorded in control solution and in the presence of melatonin assume the same values at holding potentials more negative than -120 mV and test potentials more positive than $+40$ mV. In addition, the midpoint of activation ($V_{1/2,a}$) was the same in the presence and absence of melatonin. This means that melatonin does not reduce the current by shifting the voltage-dependence of gating similarly to the action of HaTx on *drk1* K^+ channels (Swartz and MacKinnon, 1997a, b). Thus, the reduction of the conductance is the consequence of block of potassium channels.

Melatonin block is voltage-independent

We studied the voltage dependence of block by analyzing the instantaneous tail currents in the presence and absence of melatonin. We showed in single-channel experiments

(Fig. 6) that melatonin block is extremely fast, therefore the amplitude of the instantaneous tail current measured at the beginning of the test pulse following the activating pulse is a true measure of the number of channels not blocked by melatonin at that particular voltage. If melatonin block were voltage-dependent, the shape of the open channel current-voltage function obtained in the presence of melatonin would differ in shape from that obtained without melatonin. In our case the current-voltage functions were linear, and those recorded in the presence of melatonin were the scaled-down versions of those recorded under control conditions, meaning that the block by melatonin is voltage-independent (Fig. 4).

However, at test potentials below $+40$ mV the block is virtually voltage-dependent. We reported an increased slope factor (s_a) of the Boltzmann function fitted to the normalized conductance-voltage relationship (Fig. 3 A) in the presence of melatonin. We do not understand at this moment the nature of change in s_a . If melatonin bound to the closed state of the channel with higher affinity we would expect a shift in $V_{1/2,a}$ without changing s_a (Hille, 1992). Melatonin-induced alteration of the equivalent gating charge would change both $V_{1/2,a}$ and s_a . We think, therefore, that change in s_a might reflect changes in the gating of channels that are not blocked by melatonin. We believe that this effect of melatonin is independent of binding to its receptor mediating channel block.

The increase in s_a , however, can explain the left shift in the voltage dependence of steady-state inactivation (h_∞ curve). Fig. 3 A shows that the voltage dependence of normalized steady-state activation displays lower activation threshold and higher values below $V_{1/2,a}$ in the presence of melatonin as compared to control. Since inactivation of Kv1.3 is linked to the activation pathway (Marom and Levitan, 1994; Decoursey, 1990; Panyi et al., 1995), a shift in the h_∞ curve is expected in the presence of melatonin. Indeed, Fig. 3 B shows that the shift in the h_∞ curve is comparable to the shift in the activation threshold predicted by the fit of Boltzmann distribution to the points shown in Fig. 3 A.

Melatonin block and the gating state of Kv1.3

A key issue in the interpretation of the dose response curve shown in Fig. 10 is that the block is state- and voltage-independent. This was addressed in several experiments in the paper. The voltage dependence of the block was addressed above.

Several results support that the open-to-inactivated transition is not critical for melatonin block. 1) A quantitatively identical degree of block was achieved regardless of the length of the depolarizing pulse (50 ms vs. 1000–2000 ms) and the concomitant degree of inactivation at the end of the pulse (~ 20 –25% vs. $>90\%$). 2) During repetitive depolarizations with long pulses, causing high degrees of inactiva-

tion (>95%), the block of potassium current did not accumulate from pulse to pulse in the continuous presence of melatonin (Fig. 2 C). 3) As compared to the wild-type current the inactivation of the H399Y mutant current is very slow and multiexponential (Fig. 13 A). This dramatic difference in the inactivation behavior of the mutant channels is not associated with any significant influence on melatonin binding (Fig. 13 B).

Melatonin block does not accumulate in the closed state of the channels either (Fig. 9). Application of melatonin to the closed channels for several minutes (protocol B in Fig. 9) resulted in current block similar to the one determined right after the start of melatonin application (protocol A in Fig. 9).

Our single-channel results, however, do not exclude the possibility of open state block with very high block rate. The fact that the unitary current is reduced in the presence of melatonin (Fig. 6) is compatible with this scenario. Our interpretation of the reduction in the average single-channel current amplitude is that the transition between the conducting (no melatonin bound) and the nonconducting (melatonin bound) states is very fast, so that blocked periods are too brief to be resolvable using our recording apparatus. Instead, an average of the currents from the open and blocked periods is recorded, similarly to the block of *Shaker* K⁺ channels by TEA (Spruce et al., 1987).

Results discussed above do not provide sufficient evidence for preferential association of melatonin with the closed, open, or inactivated state of Kv1.3. Regardless of melatonin binding to either the closed or open states of the channel, the fast rates of block and unblock indicated by single-channel data provide instantaneous equilibration of melatonin-bound and melatonin-free states. Thus, reduction of the peak currents in the presence of melatonin indicates equilibrium block of channels and therefore dose response curves shown in Fig. 10 can be analyzed.

Modulation of inactivation

Binding of TEA to the pore of open K⁺ channels and inactivation are mutually exclusive; TEA-blocked channels cannot inactivate. This, in combination with the fast block-unblock rates, results in a decrease in the rate of macroscopic current inactivation in the presence of TEA (Grissmer and Cahalan, 1989). In contrast, melatonin speeds C-type inactivation of Kv1.3 in a concentration-dependent fashion (Figs. 2 and 7). The values of τ_v/τ_c (Fig. 7) obtained at different melatonin concentrations show significant correlation ($r = -0.923$, $p = 0.009$) with the blocked fraction of the current (calculated from the remaining fraction of current shown in Fig. 10). This means that larger fractions of melatonin-bound channels lead to faster inactivation. Thus, our interpretation of the increased inactivation rate of the current in the presence of melatonin is that melatonin-bound channels inactivate faster and melatonin binding may

modulate the cooperative interaction between subunits leading to C-type inactivation (Panyi et al., 1995). We do not currently know the relationship between the inactivation kinetics and the number of melatonin molecules bound to the channels. At the same time the kinetics of recovery from inactivation was the same regardless of the presence or absence of melatonin (Fig. 8). The simplest interpretations compatible with our results are that melatonin does not bind to the inactivated state of the channels or melatonin remains bound but does not affect the kinetics of recovery from inactivation.

Four independent melatonin binding sites

All of the results discussed above support the idea that peak currents measured in the presence of melatonin represent equilibrium block of Kv1.3 channels. Accordingly, the dose-response curve constructed from peak currents measured at 0.5–10 mM extracellular melatonin was analyzed in Fig. 10. The simplest 1:1 melatonin to channel stoichiometry model gave a poor fit to the measured data, especially at higher concentrations. Although multiple amino acid side chains located on different subunits of a tetrameric channel (MacKinnon, 1991) contribute to the formation of a single binding site for ChTx (Goldstein et al., 1994) and TEA (Heginbotham and MacKinnon, 1992), the dose response curves are well described using 1:1 stoichiometry of binding for these blockers. Thus, we proposed three other models with four *independent* binding sites for melatonin on each channel to account for the observed dose response curve. In this respect the binding of melatonin to the channel is similar to that of HaTx (Swartz and MacKinnon, 1997a, b). However, our experiments showed that melatonin, unlike HaTx, fully blocks the channel even if only a single molecule binds to it. The binding of a second, third, or fourth molecule has no further effect on the channel conductance. This model (IIa) was chosen as the best based on its lowest residual sum of squares when compared with experimental data. The other three models investigated were clearly inferior in this respect.

The validity of model IIa could be further tested by recording the washout kinetics of the drug. If melatonin were applied at a concentration close to saturation, when nearly 100% of the sites are occupied, the washout kinetics of the current would follow a sigmoidal time course (Swartz and MacKinnon, 1997a). In practice, however, we could not use this experiment to prove the validity of our model for two reasons. First, due to the fast off-rate of the drug the recovery of the current from melatonin block is much faster than the recovery of the channels from inactivation (Levy and Deutsch, 1996). Thus, if we tried to resolve washout kinetics by frequent pulsing, cumulative inactivation would develop (Marom and Levitan, 1994). Second, to saturate 95% of the binding sites melatonin should be applied at >100 times the half-blocking concentration. Due to the

high dissociation constant this would yield an irrationally concentrated drug solution.

Single-channel experiments also argue against stepwise decreases in the single-channel conductance induced by binding of individual melatonin molecules (model IIc). In case of stepwise changes in the conductance one would expect multiple peaks in the all-points histogram in the presence of melatonin. If those peaks were not distinguishable due to the small single-channel currents and large standard deviations one should observe an apparent increase in the standard deviation of the Gaussian distribution fitted to the conducting state. In contrast, the all-points histogram in the presence of melatonin has a single peak corresponding to the conducting state with reduced mean but identical standard deviation to the control (Fig. 6).

In light of our best-fitting model to the dose response curve (model IIa) very fast transitions between 0 or 1 melatonin-bound (blocked) states are responsible for reduced single-channel current in the presence of melatonin. Using model IIa, at 5 mM melatonin concentration 50% of the channels have 0 or 1 melatonin molecule bound and therefore participate in such transitions.

Avdonin and Hoshi reported recently that indole, a structural analog of melatonin (indole gives the backbone of melatonin, Fig. 1), inhibits *Shaker* potassium channels with a 4:1 drug-to-channel stoichiometry, similarly to melatonin (Avdonin and Hoshi, 2000). This strongly supports our conclusions for the existence of four independent binding sites.

Where is the melatonin binding site?

The following lines of evidence support that the binding site for melatonin is located on the extracellular surface of the channels: 1) block develops instantly after the start of melatonin application to the extracellular solution. In contrast, membrane-permeable drugs blocking potassium channels from the intracellular side often require several minutes to reach equilibrium block (Snyders et al., 1991; Snyders and Chaudray, 1996; Kirsch and Drewe, 1993). The washout kinetics for these blockers is also slow (>10 min), which is in clear contrast to our findings that relief of melatonin block is instantaneous after switching to drug-free extracellular solution. 2) The presence of melatonin in the pipette solution (1.5 mM) did not influence the reduction of whole-cell peak currents by extracellular application of 1.5 mM melatonin. If melatonin were binding to the cytosolic surface of the channels, then the effect of extracellular application of melatonin would be diminished or absent in the presence of melatonin in the pipette solution, but our results show just the opposite.

Simultaneous application of ChTx and melatonin showed that these two agents can bind independently to Kv1.3. ChTx binds to the extracellular vestibule of *Shaker* potassium channels and prevents the access of TEA, a small pore

blocker ($\sim 8 \text{ \AA}$ in diameter; Kavanaugh et al., 1991) to its binding site, i.e., their binding is mutually exclusive (Goldstein and Miller, 1993). Thus, the melatonin binding site should be outside the pore, and most likely outside the footprint of close contact residues between ChTx and the channel vestibule, which primarily influence ChTx binding (Goldstein et al., 1994). In addition, Fig. 5 shows that inward and outward currents are blocked to the same extent by melatonin. If melatonin were a pore-blocker, then interaction of the blocker with permeant ions would be expected (Demo and Yellen, 1991; Hille, 1992). This was not the case for melatonin (Fig. 5).

Allosteric interaction of melatonin and TEA binding

We found that the simultaneous presence of melatonin and TEA decreased the affinity of these drugs for Kv1.3. The following lines of evidence support that this is an allosteric modulation of separate (nonoverlapping) binding sites: 1) the relative K_d value for melatonin in the presence of different concentrations of TEA clearly deviates from pure competitive binding (Fig. 12); 2) simultaneous occupancy of ChTx and melatonin binding sites is possible (see above); however, ChTx and TEA compete for the same or overlapping binding sites.

We propose that allosteric modification of the TEA binding site by melatonin contributes to the modulation of inactivation kinetics of Kv1.3 in the presence of melatonin. The nature of amino acid side chains and their physical state at the TEA binding site (position 399) dramatically influence the rate and extent of inactivation in *Shaker* potassium channels and TEA affinity. Mutations at the TEA binding site can speed up, slow down, or even disrupt C-type inactivation (López-Barneo et al., 1993). Thus, the increased inactivation rate of Kv1.3 could be, at least partially, attributed to the effect of melatonin on critical residues determining C-type inactivation.

In conclusion, we described a unique pattern of interactions of melatonin with Kv1.3 channels leading to the block of K^+ current. The block was state- and voltage-independent (in a certain region of the voltage axis) and was not compatible with either the pore occlusion mechanism or the gating modifier mechanism described in the literature. Furthermore, the best fit to the dose response curve suggested that four independent binding sites existed for melatonin and the occupancy of one of these sites was sufficient for full block of the channels. These effects of melatonin were purely pharmacological because the doses applied in this study were several orders of magnitude higher than the peak serum melatonin concentration in humans; however, structural analogs of melatonin with much higher affinity for Kv1.3 might serve as templates for drug development. Similarly, several non-peptide inhibitors of Kv1.3 were reported

recently with potential therapeutic consequences. Further experiments are planned to elucidate the details of the blocking mechanism and location of the binding site of melatonin.

APPENDIX

To determine whether melatonin and TEA compete for overlapping binding sites we had to calculate how the relative K_d value would change as a function of TEA concentration if there were competition between them.

If the assumptions that one bound melatonin molecule prevents TEA from binding and bound TEA prevents melatonin from binding are made, the conducting fraction of channels can be determined. If melatonin bound to the channel in a 1:1 manner, similarly to TEA, the respective dissociation constants would be

$$K_d^{\text{TEA}} = \frac{[\text{O}][\text{TEA}]}{[\text{O} + \text{TEA}]} \quad \text{and} \quad K_d^{\text{m},1:1} = \frac{[\text{O}][\text{m}]}{[\text{O} + \text{m}]}$$

In the equation $[\text{m}]$ is the melatonin and $[\text{TEA}]$ is the TEA concentration, $[\text{O} + \text{TEA}]$, $[\text{O} + \text{m}]$, and $[\text{O}]$ represent the fraction of channels blocked by TEA, blocked by melatonin, and not blocked by either compound, respectively. $K_d^{\text{m},1:1}$ represents the theoretical dissociation constant of melatonin in a 1:1 interaction.

Since $[\text{O}] + [\text{O} + \text{TEA}] + [\text{O} + \text{m}] = 1$, the remaining fraction (RF) of the whole-cell current would be given by

$$RF = \frac{1}{[\text{TEA}]/K_d^{\text{TEA}} + [\text{m}]/K_d^{\text{m},1:1} + 1}$$

This equation does not account for the four binding sites. To replace $K_d^{\text{m},1:1}$ by the real individual dissociation constant (K_d^{m}) one must ask the question: at what $[\text{m}]/K_d^{\text{m}}$ ratio will the 4:1 stoichiometry formula yield the same RF as the 1:1 stoichiometry formula at $[\text{m}]/K_d^{\text{m},1:1}$ ratio in the presence of melatonin alone? The relationship is the following:

$$\frac{[\text{m}]}{K_d^{\text{m},1:1}} = \left(1 + \frac{[\text{m}]}{K_d^{\text{m}}}\right)^4 - 1$$

Thus, if the above substitution is made, the remaining fraction of the whole-cell current becomes

$$RF = \frac{1}{[\text{TEA}]/K_d^{\text{TEA}} + (1 + [\text{m}]/K_d^{\text{m}})^4}$$

where $K_d^{\text{TEA}} = 11.1$ mM and $K_d^{\text{m}} = 8.11$ mM. Solving the equation for $[\text{m}]$ we get

$$[\text{m}] = \left(\frac{1}{RF} - \frac{[\text{TEA}]}{K_d^{\text{TEA}}}\right)^{1/4} K_d^{\text{m}}$$

The melatonin concentration that reduces the current amplitude by 50% (taking the current in the presence of TEA alone as 100%) at any TEA concentration can be calculated using the formula. In this case RF will be half of what it would be in the presence of TEA alone, thus

$$RF = \frac{K_d^{\text{TEA}}}{2(K_d^{\text{TEA}} + [\text{TEA}])}$$

With this substitution the equation becomes

$$[\text{m}] = \left(\left(2 + \frac{[\text{TEA}]}{K_d^{\text{TEA}}}\right)^{1/4} - 1\right) K_d^{\text{m}}$$

From this half-blocking melatonin concentration an apparent K_d value can be determined, which will be greater than the actual 8.11 mM. The relative K_d value is the ratio of this apparent and real K_d values. This is plotted in Fig. 12 as a function of TEA concentration.

The kind gifts of Professor Carol Deutsch, University of Pennsylvania (pRc/CMV/H399Y, Ccd4neo) are highly appreciated.

The authors thank Professor Dirk L. Ypey for critical reading of the manuscript.

This work was supported by the following grants: OTKA T23873, F035251, and T29947; ETT T05/102/2000; MAKAF JF 542; FIRCA 1R03TW0722; FKFP 327/2000 and 0622/2000 (to D.S., R.G., and G.P.).

REFERENCES

- Aiyar, J., J. M. Withka, J. P. Rizzi, D. H. Singleton, G. C. Andrews, W. Lin, J. Boyd, D. C. Hanson, M. Simon, B. Dethlefs, C. Lee, J. E. Hall, G. A. Gutman, and K. G. Chandy. 1995. Topology of the pore-region of a K^+ channel revealed by the NMR-derived structures of scorpion toxins. *Neuron*. 15:1169–1181.
- Avdonin, V. B., and T. Hoshi. 2000. Potassium channel block by indole. *Biophys. J.* 78:212a. (Abstr.).
- Cahalan, M. D., K. G. Chandy, T. E. Decoursey, and S. Gupta. 1985. A voltage-gated potassium channel in human T lymphocytes. *J. Physiol. (Lond)*. 358:197–237.
- Cahalan, M. D., and R. S. Lewis. 1990. Functional roles of ion channels in lymphocytes. *Semin. Immunol.* 2:107–117.
- Costa, E. J., R. H. Lopes, and M. T. Lamy Freund. 1995. Permeability of pure lipid bilayers to melatonin. *J. Pineal Res.* 19:123–126.
- Decoursey, T. E. 1990. State-dependent inactivation of K^+ currents in rat type II alveolar epithelial cells. *J. Gen. Physiol.* 95:617–646.
- Decoursey, T. E., K. G. Chandy, S. Gupta, and M. D. Cahalan. 1984. Voltage-gated K^+ channels in human T lymphocytes: a role in mitogenesis? *Nature*. 307:465–468.
- Demo, S. D., and G. Yellen. 1991. The inactivation gate of the *Shaker* K^+ channel behaves like an open-channel blocker. *Neuron*. 7:743–753.
- Deutsch, C., and L.-Q. Chen. 1993. Heterologous expression of specific K^+ channels in T lymphocytes: functional consequences for volume regulation. *Proc. Natl. Acad. Sci. U.S.A.* 90:10036–10040.
- Deutsch, C., D. Krause, and S. C. Lee. 1986. Voltage-gated potassium conductance in human T lymphocytes stimulated with phorbol ester. *J. Physiol. (Lond)*. 372:405–423.
- Deutsch, C., M. Price, S. Lee, V. F. King, and M. L. Garcia. 1991. Characterization of high affinity binding sites for charybdotoxin in human T lymphocytes. Evidence for association with the voltage-gated K^+ channel. *J. Biol. Chem.* 266:3668–3674.
- Goldstein, S. A., and C. Miller. 1993. Mechanism of Charybdotoxin block of a voltage-gated K^+ channel. *Biophys. J.* 65:1613–1619.
- Goldstein, S. A., D. J. Pheasant, and C. Miller. 1994. The Charybdotoxin receptor of a *Shaker* K^+ channel: peptide and channel residues mediating molecular recognition. *Neuron*. 12:1377–1388.
- Grissmer, S., and M. D. Cahalan. 1989. TEA prevents inactivation while blocking open K^+ channels in human T lymphocytes. *Biophys. J.* 55:203–206.
- Grissmer, S., A. N. Nguyen, and M. D. Cahalan. 1993. Calcium-activated potassium channels in human T lymphocytes. *Biophys. J.* 64:3a. (Abstr.).
- Heginbotham, L., and R. MacKinnon. 1992. The aromatic binding site for tetraethylammonium ion on potassium channels. *Neuron*. 8:483–491.

- Hille, B. 1992. *Ion Channels of Excitable Membranes*. Sinauer Associates Inc., Sunderland, MA.
- Jiang, Z. G., C. S. Nelson, and C. N. Allen. 1995. Melatonin activates an outward current and inhibits Ih in rat suprachiasmatic nucleus neurons. *Brain Res.* 687:125–132.
- Kavanaugh, M. P., M. D. Varnum, P. B. Osborne, M. J. Christie, A. E. Busch, J. P. Adelman, and R. A. North. 1991. Interaction between tetraethylammonium and amino acid residues in the pore of cloned voltage-dependent potassium channels. *J. Biol. Chem.* 266:7583–7587.
- Kirsch, G. E., and J. A. Drewe. 1993. Gating-dependent mechanism of 4-aminopyridine block in two related potassium channels. *J. Gen. Physiol.* 102:797–816.
- Kirsch, G. E., M. Tagliatela, and A. M. Brown. 1991. Internal and external TEA block in single cloned K⁺ channels. *Am. J. Physiol.* 261:583–590.
- Lee, S. C., D. I. Levy, and C. Deutsch. 1992. Diverse K⁺ channels in primary human T lymphocytes. *J. Gen. Physiol.* 99:771–793.
- Levy, D. I., and C. Deutsch. 1996. Recovery from C-type inactivation is modulated by extracellular potassium. *Biophys. J.* 70:798–805.
- Liebmann, P. M., A. Wölfler, P. Felsner, D. Hofer, and K. Schauenstein. 1997. Melatonin and the immune system. *Int. Arch. Allergy Immunol.* 112:203–211.
- López-Barneo, J., T. Hoshi, S. H. Heinemann, and R. W. Aldrich. 1993. Effects of external cations and mutations in the pore region on C-type inactivation of Shaker potassium channels. *Receptors and Channels.* 1:61–71.
- MacKinnon, R. 1991. Determination of the subunit stoichiometry of a voltage-activated potassium channel. *Nature.* 350:232–235.
- MacKinnon, R., and C. Miller. 1988. Mechanism of charybdotoxin block of the high-conductance, Ca²⁺-activated K⁺ channel. *J. Gen. Physiol.* 91:335–349.
- MacKinnon, R., and G. Yellen. 1990. Mutations affecting TEA blockade and ion permeation in voltage-activated K⁺ channels. *Science.* 250:276–279.
- Malayev, A. A., D. J. Nelson, and L. H. Phillipson. 1995. Mechanism of clofilium block of the human Kv1.5 delayed rectifier potassium channel. *Mol. Pharmacol.* 47:198–205.
- Marom, S., and I. B. Levitan. 1994. State-dependent inactivation of the Kv3 potassium channel. *Biophys. J.* 67:579–589.
- Matteson, D. R., and C. Deutsch. 1984. K⁺ channels in T lymphocytes: a patch clamp study using monoclonal antibody adhesion. *Nature.* 307:468–471.
- Miller, C. 1988. Competition for block of a Ca²⁺-activated K⁺ channel by charybdotoxin and tetraethylammonium. *Neuron.* 1:1003–1006.
- Motulsky, H. J., and L. A. Ransnas. 1987. Fitting curves to data using nonlinear regression: a practical and nonmathematical review. *FASEB J.* 1:365–374.
- Oreslock, J. P. 1984. The pineal gland: basic and clinical correlations. *Endocr. Rev.* 5:282–297.
- Panyi, G., and C. Deutsch. 1997. Anomalous inactivation of a Kv1.3 mutant. *Biophys. J.* 72:27a. (Abstr.).
- Panyi, G., Z.-F. Sheng, L.-W. Tu, and C. Deutsch. 1995. C-type inactivation of a voltage-gated K⁺ channel occurs by a cooperative mechanism. *Biophys. J.* 69:896–904.
- Persengiev, S. P., and S. Kyurkchiev. 1993. Selective effect of melatonin on the proliferation of lymphoid cells. *Int. J. Biochem.* 25:441–444.
- Péter, M., Z. Varga, G. Panyi, L. Bene, S. Damjanovich, C. Pieri, L. D. Possani, and R. Gáspár. 1998. *Pandinus imperator* scorpion venom blocks voltage-gated K⁺ channels in human lymphocytes. *Biochem. Biophys. Res. Commun.* 242:621–625.
- Pieri, C., R. Recchioni, F. Moroni, F. Marcheselli, M. Marra, S. Marioni, and R. Di-Primio. 1998. Melatonin regulates the respiratory burst of human neutrophils and their depolarization. *J. Pineal Res.* 24:43–49.
- Pioli, C., M. C. Caroleo, G. Nistico, and G. Doria. 1993. Melatonin increases antigen presentation and amplifies specific and nonspecific signals for T-cell proliferation. *Int. J. Immunopharmacol.* 15:463–468.
- Rasmusson, R. L., Y. Zhang, D. L. Campbell, M. B. Comer, R. C. Castellino, S. Liu, and H. C. Strauss. 1995. Bi-stable block by 4-aminopyridine of a transient K⁺ channel (Kv1.4) cloned from ferret ventricle and expressed in *Xenopus* oocytes. *J. Physiol.* 485:59–71.
- Snyders, D. J., and A. Chaudray. 1996. High affinity open channel block by dofetilide of HERG expressed in a human cell line. *Mol. Pharmacol.* 49:949–955.
- Snyders, D. J., K. M. Knoth, S. L. Roberds, and M. M. Tamkun. 1991. Time-, voltage-, and state-dependent block by quinidine of a cloned human cardiac potassium channel. *Mol. Pharmacol.* 41:322–330.
- Spruce, A. E., N. B. Standen, and P. R. Stanfield. 1987. The action of external tetraethylammonium ions on unitary delayed rectifier potassium channels of frog skeletal muscle. *J. Physiol. Lond.* 393:467–478.
- Swartz, K. J., and R. MacKinnon. 1997a. Hanatoxin modifies the gating of a voltage-dependent K⁺ channel through multiple binding sites. *Neuron.* 18:665–673.
- Swartz, K. J., and R. MacKinnon. 1997b. Mapping the receptor site for Hanatoxin, a gating modifier of voltage-dependent K⁺ channels. *Neuron.* 18:675–682.
- Varga, Z., M. Péter, G. Panyi, C. Pieri, S. Damjanovich, and R. Gáspár. 1999. Molecular pharmacological effects of melatonin on K⁺ channels of human T-lymphocytes. *Biophys. J.* 76:76a. (Abstr.).
- Vijayalaxmi, R. J. Reiter, B. Z. Leal, and M. L. Meltz. 1996. Effect of melatonin on mitotic and proliferation indices, and sister chromatid exchange in human blood lymphocytes. *Mutat. Res.* 351:187–192.
- Wanecek, J., and D. C. Klein. 1992. Sodium-dependent effects of melatonin on membrane potential of neonatal rat pituitary cells. *Endocrinology.* 131:939–946.
- Yellen, G., M. E. Jurman, T. Abramson, and R. MacKinnon. 1991. Mutations affecting internal TEA blockade identify the probable pore-forming region of a K⁺ channel. *Science.* 251:939–942.